NACA

RESEARCH MEMORANDUM

THE EFFECTS OF OSCILLATION AMPLITUDE AND FREQUENCY ON THE EXPERIMENTAL DAMPING IN PITCH OF A TRIANGULAR WING HAVING AN ASPECT RATIO OF 4

By Benjamin H. Beam

Ames Aeronautical Laboratory
Moffett Field, Calif.

NATIONAL ADVISORY COMMITTEE
FOR AERONAUTICS

WASHINGTON
September 5, 1952

Classification cancelled (or changed to Unclassified)

By Authority of NASA Tech Pub Announcement #104
(OFFICER AUTHORIZED TO CHANGE)

By 3 Aug 66

(GRADE OF OFFICER MAKING CHANGE)

5 Apr. 67
DATE

NATIONAL ADVISORY COMMITTEE FOR AERONAUTICS

RESEARCH MEMORANDUM

THE EFFECTS OF OSCILLATION AMPLITUDE AND FREQUENCY ON THE EXPERIMENTAL DAMPING IN PITCH OF A TRIANGULAR WING HAVING AN ASPECT RATIO OF 4

By Benjamin H. Beam

SUMMARY

The results are presented of a wind-tunnel investigation of the damping in pitch of a model triangular wing having an aspect ratio of 4 combined with a slender pointed body. The investigation was conducted at Mach numbers from 0.10 to 0.95 for Reynolds numbers of 550,000 and 1,250,000 with additional data obtained at Reynolds numbers of 3,000,000 and 6,000,000 at a Mach number of 0.23. Reduced oscillation frequencies ranged from 0.031 to 0.069 at high Mach numbers and from 0.11 to 0.28 at low Mach numbers. Data were obtained for angles of attack from 0° to 19° and for steady-state oscillation amplitudes from 1° to 4° using a feedback-controlled, forced-oscillation technique described herein.

The results show a large effect of Reynolds number for certain test conditions and a region of dynamic instability at high subsonic Mach numbers. Effects of oscillation amplitude and frequency were found to be of secondary importance except at high subsonic Mach numbers. The results of this investigation are shown to agree with values of the damping-in-pitch coefficient measured by the free-oscillation technique for similar test conditions.

INTRODUCTION

Increasing attention is being directed to the dynamic characteristics of aircraft. One reason for this is that present-day high flight speeds require correspondingly faster and more precise aircraft control which may be considerably affected by the dynamics of the aircraft. In addition, the trend toward high flight altitudes and tailless aircraft configurations has resulted in decreased aerodynamic damping. The need

[redacted]

for adequate information on aerodynamic damping is particularly acute in the transonic Mach number range.

The damping of the short-period longitudinal oscillations of an aircraft is to a large degree dependent upon the damping of single-degree-of-freedom pitching oscillations about the aircraft center of gravity. Experimental results have been presented in reference 1 for several triangular wing configurations in which the damping was obtained from measurements of the logarithmic decrement of single-degree-of-freedom pitching oscillations in a wind tunnel. Following this investigation and its evidence of dynamic instability at transonic Mach numbers, a device was built for measuring the damping in pitch of wind-tunnel models by a single-degree-of-freedom forced-oscillation technique. This equipment could be used to measure damping under unstable aerodynamic conditions and also permitted the systematic investigation of the effects of frequency and amplitude.

The purpose of this report is to present data showing the effects on the damping in pitch caused by variations in Mach number, Reynolds number, angle of attack, frequency, oscillation amplitude, and longitudinal position of the pitching axis as measured with the forced-oscillation apparatus. A comparison with damping-in-pitch coefficients determined by the free-oscillation technique (reference 1) is also presented.

SYMBOLS

$C_{m_q}+C_{m_{\dot{\alpha}}}$ wind-tunnel damping-in-pitch coefficient[1] $\left(-\frac{4\mu}{\rho V S \bar{c}^2}\right)$

[1]For linear operation C_{m_q} and $C_{m_{\dot{\alpha}}}$ correspond to the theoretically derived coefficients:

$$C_{m_q} = \left(\frac{C_m}{q\bar{c}/2V}\right)_{q \to 0} \qquad C_{m_{\dot{\alpha}}} = \left(\frac{C_m}{\dot{\alpha}\bar{c}/2V}\right)_{\dot{\alpha} \to 0}$$

where

C_m pitching-moment coefficient referred to the pitching axis $\left(\frac{\text{pitching moment}}{\frac{1}{2}\rho V^2 S\bar{c}}\right)$

q angular pitching velocity, radians per second

$\dot{\alpha}$ time rate of change of angle of attack, radians per second

A_r real part of feedback loop-transfer function, foot-pounds-seconds

A_i imaginary part of feedback loop-transfer function, foot-pounds-seconds

I mass moment of inertia of model, slug-feet squared

$J_n'(\xi)$ derivative with respect to ξ of the Bessel function of the first kind of order n and argument ξ

M free-stream Mach number $\left(\frac{V}{a}\right)$

R wind-tunnel test-section radius, feet

RN Reynolds number $\left(\frac{V\bar{c}\rho}{\lambda}\right)$

S model wing area, square feet

T instantaneous value of feedback torque, foot-pounds

V free-stream airspeed, feet per second

a free-stream speed of sound, feet per second

b wing span, feet

$\bar{c}$ wing mean aerodynamic chord $\left(\frac{2}{S}\int_0^{b/2} c^2 dy\right)$, feet

c local wing chord, feet

e base of natural logarithms

f oscillation frequency, cycles per second

i $\sqrt{-1}$

k restoring moment per unit angular deflection, foot-pounds per radian

t time, seconds

x_r chordwise distance from the leading edge of the mean aerodynamic chord to the pitching axis, feet

[redacted]

y	spanwise distance from plane of symmetry, feet
α_o	static angle of attack of wing chord line, degrees
θ	instantaneous angular deflection of the model from its static position, radians
θ_{max}	maximum angular deflection of the model from its static position, radians except where noted
$\dot{\theta},\ddot{\theta}$	$\frac{d\theta}{dt}, \frac{d\theta^2}{dt^2}$
λ	absolute viscosity of air, slugs per foot-second
μ	aerodynamic damping moment per time rate of change of angular deflection, foot-pounds-seconds
μ_1	mechanical damping moment per time rate of change of angular deflection, foot-pounds-seconds
ρ	mass density of air, slugs per cubic foot
ω	angular frequency of pitching oscillation ($2\pi f$), radians per second

DESCRIPTION OF TEST EQUIPMENT

Oscillator

A schematic sketch of the oscillator is shown in figure 1. Essentially it is a feedback oscillator loop which is composed of electrical and mechanical elements. The output of the oscillator is damping torque of either positive or negative sign about the pitching axis of the model. When the model is oscillating at a steady-state amplitude, the damping torque supplied by the oscillator is of equal magnitude and opposite sign to the damping torque supplied by the aerodynamic and mechanical-hysteresis effects.

The model and its crossed-flexure-pivot support form a single-degree-of-freedom oscillatory system which serves as the tuning element of the oscillator. A change of natural frequency is accomplished by changing the dimensions of the flexure pivots. Any angular motion of the model is transmitted through the push rod to the velocity pickup. The signal from the velocity pickup is then amplified in the feedback

loop and used to drive the mechanical system by means of the electromagnetic shaker. The phase relation of the feedback force to the model oscillation is such as to either increase or decrease the oscillation amplitude depending on whether the feedback is positive or negative.

It is seen that for positive feedback with sufficient gain, oscillations will build up from rest even though the model is positively damped aerodynamically. For negative feedback with sufficient gain, oscillations can be made to die out even though the model is aerodynamically unstable. To stabilize the steady-state amplitude at a desired level a thermister was used.[2] A thermister is a resistance element which has the important nonlinear property that although its resistance changes with temperature, or the root-mean-square value of the current through it, its resistance is practically constant over one cycle and thus the wave form of the oscillation is undistorted.

The mathematical relations that apply for the model and the oscillator can be developed from the equation of motion for a single-degree-of-freedom oscillation (reference 3)

$$I\ddot{\theta} + (\mu+\mu_1)\,\dot{\theta} + k\theta = T \qquad (1)$$

For steady-state sinusoidal oscillations $\theta = \theta_{max}\, e^{i\omega t}$ and the left side of equation (1) reduces to

$$-I\omega^2\,\theta + i\omega\,(\mu+\mu_1)\,\theta + k\theta$$

The right side of equation (1) represents the torque fed back into the oscillation. For most efficient operation T should be exactly in phase or 180° out of phase with $\dot{\theta}$, but this is not a necessary condition. In general, T is related to $\dot{\theta}$ by the transfer function of the entire feedback loop and is a complex quantity. Since the transfer function is not affected by variations of instantaneous amplitude at any given frequency and feedback gain, it can be reduced to the form

$$T = (A_r+iA_i)\,\dot{\theta} = i\omega\,(A_r+iA_i)\,\theta$$

Equation (1) can then be written

$$[k-\omega^2 I+\omega A_i]\,\theta + i\omega\,[\mu+\mu_1-A_r]\,\theta = 0 \qquad (2)$$

---

[2]For a short discussion and bibliography on this subject see reference 2.

In equation (2) both the real and imaginary parts must equal zero. The real part determines the frequency of oscillation

$$\omega = + \frac{A_i}{2I} \pm \sqrt{\frac{A_i^2}{4I^2} + \frac{k}{I}} \tag{3}$$

In the present case, a comparison of the open-loop oscillation frequency with the closed-loop oscillation frequency revealed that the terms in equation (3) containing A_i were negligible compared with $\sqrt{k/I}$ so the frequency of oscillation becomes simply

$$\omega = \sqrt{\frac{k}{I}} \tag{4}$$

The imaginary part of equation (2), which represents the sum of the damping moments, can be rearranged into the form

$$(\mu+\mu_1)\ \dot{\theta} = A_r\ \dot{\theta} \tag{5}$$

The term on the right in equation (5) represents the component of feedback torque which is in phase with $\dot{\theta}$. For any particular frequency it is proportional to the feedback-signal current flowing in the armature circuit of the shaker under constant field excitation. From equation (5)

$$\mu = \frac{(A_r\dot{\theta})}{\dot{\theta}} - \mu_1 \tag{6}$$

and by definition

$$C_{m_q} + C_{m_{\dot{\alpha}}} = - \frac{4\mu}{\rho V S \bar{c}^2} \tag{7}$$

Equations (6) and (7) were used to determine the damping-in-pitch coefficients in this report. The term A_r was actually never evaluated since the product $A_r\dot{\theta}$ could be obtained directly from the shaker armature current and a calibration of the damping-torque-current ratio for the range of test frequencies. The oscillation velocity, $\dot{\theta}$, was obtained from the voltage output of the velocity pickup and a calibration of the voltage-velocity ratio. For both calibration and test purposes, the frequency of oscillation was determined by synchronizing a calibrated, variable-frequency oscillator with the output of the mechanical oscillator. The mechanical damping term, μ_1, was obtained from a wind-off calibration for which μ becomes zero in equation (6).

[redacted]

The calibrations for $\dot{\theta}$ and $A_r\dot{\theta}$ referred to above were conducted on a test stand prior to installation in the wind tunnel with a calibration bracket in place of the model. Damping torque was introduced into the oscillating system by means of a crank arm from a second electromagnetic shaker in which the armature was short circuited. The damping torque, $A_r\dot{\theta}$, for a given oscillation velocity was calculated from the short-circuit current and the armature resistance of the second shaker. The oscillation amplitude was measured by the angular deflection of the center line of the calibration bracket and this, with the frequency, determined the oscillation velocity, $\dot{\theta}$. This system provided a convenient experimental means of determining the calibration constants through the range of desired frequencies and verified the linearity of response with oscillation amplitude and feedback gain.

It is seen that the preceding analysis depends on the condition that

$$\theta = \theta_{max} e^{i\omega t}$$

or that the oscillations are sinusoidal. This requires that the coefficients in equation (1) remain constant with variations in θ, and in cases where $C_{m_q} + C_{m_{\dot{\alpha}}}$ varies with θ this requirement is not satisfied and the oscillations are not completely sinusoidal. If the damping torque is much smaller than the torques due to elastic and inertia effects, however, the wave shape of the model oscillation remains practically sinusoidal and, since the feedback signal is proportional to the rate of change of amplitude of the model oscillation, it is also practically sinusoidal. Thus, an approximately sinusoidal feedback torque is used to oppose a nonsinusoidal aerodynamic damping torque. For a steady-state oscillation the power supplied by the feedback torque must be equal and opposite to the power supplied by the aerodynamic forces (neglecting for the moment the mechanical damping effects), and this requires that the root-mean-square values of the two torques be equal. The resulting damping-in-pitch coefficient then becomes an equivalent damping-in-pitch coefficient which results in the same root-mean-square value of torque being supplied to a sinusoidal oscillation. A rough idea of the error involved in considering the oscillations to be sinusoidal can be obtained by comparing the ratio of the equivalent damping torque to the inertia torque. The maximum value of this ratio was 7.5 percent in the present case under test conditions where $C_{m_q} + C_{m_{\dot{\alpha}}}$ was not constant with θ.

With regard to the error in the electronic equipment, calculations show that the magnitude of the feedback signal for a given damping-in-pitch coefficient is proportional to the frequency, the Reynolds number,

[redacted]

the oscillation amplitude, and the absolute viscosity of air. This is illustrated by the expression for the aerodynamic damping moment

$$\mu\dot{\theta} = -\frac{1}{4}\rho V S\bar{c}^2(C_{m_q} + C_{m_{\dot{\alpha}}})\,\dot{\theta} = -i\frac{\pi}{2}\,S\bar{c}\,\lambda f(RN)\theta_{max}\,(C_{m_q} + C_{m_{\dot{\alpha}}})e^{i\omega t} \quad (8)$$

Over the range of Reynolds number, frequency, and oscillation amplitude at which tests were conducted, there was a variation in feedback-signal amplitude of approximately 75 to 1 for the same value of damping-in-pitch coefficient. The uncertainty in reading the feedback signal was estimated to be approximately 0.2 percent of the maximum feedback-signal value but, when the variation in feedback signal level with operating condition was considered, the approximate percentage uncertainty in the damping-in-pitch coefficient for a given test condition became

$$\text{Percentage uncertainty} = \frac{280{,}000{,}000}{f\theta_{max}(RN)(C_{m_q} + C_{m_{\dot{\alpha}}})} \times 0.2 \text{ percent}$$

where θ_{max} is measured in degrees. No quantitative evaluation was made of the error caused by pickup of stray electrical or mechanical vibrations in the feedback loop, but the wave shape of the feedback signal was continuously monitored by means of an oscilloscope and these effects are believed to result in errors in the damping-in-pitch coefficient of less than 5 percent.

Internal deflections of the push rod and torque transmitting mechanism were found to result in an error in the indicated oscillation amplitude of less than 5 percent from the mean over the entire operating range. Thermal effects should not change the calibration but, except for the vibration pickup, this was not verified experimentally.

Model

The model consisted of a triangular wing with an aspect ratio of 4 combined with a slender, pointed body. This model, the dimensions of which are shown in figure 2, was also used in the tests reported in reference 1 over the same Mach number range as the present tests. The wing sections were the NACA 0006-63 in planes parallel to the air stream. The model was constructed of wood over a steel spar, with brass stiffeners in the wing tips and at the base of the body.

Model Support System

A preliminary investigation of the vibration characteristics of the model support system revealed a fundamental cantilever vibration mode at approximately 28 cycles per second. This resonant condition was

undesirable because the resulting support deflections would introduce a second degree of freedom for the model and equation (1) would be invalid. Attempts to increase the stiffness of the support so that its natural frequency would be well above the range of operation were unsuccessful and it did not appear possible to do this without major alterations to the tunnel support. It was found that with a 500-pound weight suspended from the sting by a cable leading out of the test section, the fundamental cantilever mode became approximately 9 cps with a heavily damped higher mode of approximately 35 cps. Data were taken with the weight removed for frequencies of 11 and 15 cps and with the weight attached for frequencies of 15, 19, 23, and 27 cps. A photograph of the model and support with the weight cable attached is shown in figure 3.

Wind Tunnel

These tests were conducted in the Ames 12-foot pressure wind tunnel. This tunnel is of the variable pressure, closed-return type capable of attaining air-stream velocities close to the speed of sound at low Reynolds numbers, and Reynolds numbers per foot as high as 10,000,000 at low Mach numbers. The turbulence level is very low, approaching that of free air.

CORRECTIONS TO DATA

Blockage corrections have been evaluated by the method of reference 4 and applied to the Mach number and the dynamic pressure. The magnitude of these corrections is illustrated by the correction for a Mach number of 0.95, for which the uncorrected Mach number was 0.942 and the ratio of corrected to uncorrected dynamic pressure was 1.007. The estimated choking Mach number was 0.970.

Corrections for the mechanical damping of the model and oscillator in the absence of aerodynamic forces were made using data from wind-off tests after each configuration change. The effect of air damping at a wind velocity of zero was evaluated by varying the static pressure from 14.7 to 2.5 pounds per square inch absolute and was found to be negligible. The magnitudes of the wind-off damping corrections and the experimental scatter are illustrated in figure 4. Also shown in figure 4, for comparative purposes, is the value of μ which would result in a damping-in-pitch coefficient of 1.0 calculated from equation (8) for a Reynolds number of 1,250,000 and a value of absolute viscosity corresponding to a mean tunnel temperature.

[redacted]

The mechanical damping factor, μ_1, is shown in figure 4 to vary considerably with oscillation amplitude and frequency. At the lowest frequency and for oscillation amplitudes less than approximately 2°, the mechanical damping was too small to be measured with the test equipment and is shown to be zero even though some mechanical damping was always present. At the highest frequency the mechanical damping was of the same order of magnitude as the aerodynamic damping. It was also found that the wind-on oscillation frequencies differed somewhat from the wind-off frequencies because of changes in the aerodynamic restoring moment over the range of Mach numbers and angles of attack. This difference in frequency varied from a maximum of approximately 3 cps at the lowest frequency to approximately 1 cps at the highest frequency.

No correction was made for the effect of the wind-tunnel walls on the damping-in-pitch coefficients. The wind-tunnel-wall interference effects on dynamic stability derivatives have not as yet been established with certainty, and no correction was available to the author which included the effects of compressibility.

In reference 5 the possibility is suggested that aerodynamic resonance may affect the accuracy of measurement of dynamic stability coefficients at certain frequencies corresponding to the natural frequencies of the transverse oscillations of air in the wind-tunnel test section. A calculation of this effect was made for the Ames 12-foot wind tunnel in which the normal modes of the transverse oscillations of air in the circular test section were considered to be given by the various values of (reference 6)

$$J'_n\left(\frac{\omega R}{a}\right) = 0 \qquad n = 0,1,2,3 \ldots \tag{9}$$

A correction for compressibility on the basis of standing waves similar to that in reference 5 results in

$$J'_n\left(\frac{\omega R}{a\sqrt{1-M^2}}\right) = 0 \qquad n = 0,1,2,3 \ldots \tag{10}$$

The only value of equation (10) which results in resonant frequencies which coincide with test frequencies in the range of test Mach numbers is the least value for $n = 1$, for which the resonant frequency is 27 cps at a Mach number of 0.87 and 23 cps at a Mach number of 0.90. However, the oscillation mode at the resonant frequency for $n = 1$ is asymmetrical about a nodal diameter through the test section, and the analysis of reference 5 implies that where the sources of the disturbance (i.e., the oscillating model) lie on a nodal diameter, that particular mode will not affect the measured results. On this basis it was concluded that aerodynamic resonance in the test section would not affect the data of this report.

RESULTS

Six aerodynamic variables were considered for their possible effect on the magnitude of the damping-in-pitch coefficient. In addition to the three variables which affect the static characteristics, Mach number, Reynolds number, and angle of attack, three additional variables which may affect the dynamic characteristics are oscillation amplitude, oscillation frequency, and the chordwise location of the pitching axis. All these variables were investigated to some extent and the results are presented in figures 5 through 17 for which an index is presented in table I.

DISCUSSION

Effects of Oscillation Amplitude

An inspection of figures 5 and 6 reveals that at a Reynolds number of 1,250,000 and an angle of attack of zero the damping-in-pitch coefficient is essentially independent of oscillation amplitude at Mach numbers less than 0.92 for all frequencies except the highest. At the lower frequencies the damping in pitch appears to decrease slightly with increasing amplitude, while at the highest frequency it increases with amplitude. The dynamical theory of small oscillations on which most stability calculations are based involves the assumption that the various stability derivatives remain constant with variations in oscillation amplitude and, in general, the data at frequencies below 27 cps are in accord with such an assumption for Mach numbers below 0.92. The scatter in the data at Mach numbers of 0.90 and above was caused partly by variations in tunnel Mach number and partly by sporadic aerodynamic disturbances of a transient nature which made the reading of the steady-state-signal values somewhat uncertain. The data clearly show, however, that at a Mach number between 0.92 and 0.94 the damping-in-pitch coefficient abruptly shifts from a negative (or stable) value toward a positive (or unstable) value and exhibits a strong dependence on oscillation amplitude. A good example of the type of variation under discussion is shown in figure 5(d). It is interesting to note that the type of variation shown for a Mach number of 0.95 could result in low-amplitude steady-state oscillations of an aircraft in flight which, while not necessarily dangerous, might be objectionable for other reasons.

Effects of Mach Number

The curves showing the variation of the damping-in-pitch coefficient with Mach number (fig. 7) were obtained from the data in figure 5. Theory

(reference 1) indicates that the damping-in-pitch coefficient becomes more negative as the Mach number is increased which is verified by these data for Mach numbers below 0.90. For Mach numbers greater than approximately 0.90, a subsonic theory would not be expected to apply. A wind-tunnel investigation of the static longitudinal characteristics of a similar model configuration (reference 7) revealed that the drag coefficient begins to rise abruptly and the maximum lift-drag ratio decreases as the Mach number is increased above 0.90. This indicates a possible connection between static force-divergence Mach number and the Mach number at which abrupt changes occur in the damping.

In figure 8 the variation of damping-in-pitch coefficient with Mach number from the present investigation is shown compared with data obtained from a free-oscillation test (reference 1) for approximately the same test conditions. The data agree fairly well and indicate that the two methods of testing yield comparable results. Also shown in figure 8 is the calculated variation of $C_{m_q} + C_{m_{\dot{\alpha}}}$ from reference 1 for both the wing alone and wing-body combination. The theory for the wing alone is an approximate one in which the damping moments caused by lift on the wing contain a correction for aspect ratio but in which the pure moment couple arising from the effective camber of the wing chord line in pitching motion is evaluated by simple strip theory. The theory for the body indicates that its damping in pitch is small and positive; however, unsteady flow around the blunt base of the body might result in large effects on the damping for certain conditions. Nevertheless, although possibly fortuitous, the theory is shown to agree quite well with experimental data for the conditions represented in figure 8.

Effects of Reynolds Number

It was not possible to increase the Reynolds number above 1,250,000 at the high Mach numbers due to model strength limitations; however, it was possible to reduce the Reynolds number to 550,000 and the results of this change on the damping-in-pitch coefficient are shown in figure 9. The data shown in figures 9(a) and 9(b) were taken under the same test conditions and are presented to illustrate the repeatability of data taken near the beginning of the test program (fig. 9(a)) with that taken at the conclusion (fig. 9(b)). These data should be compared with that in figure 5(a) for the same frequency but a higher Reynolds number. Figure 9(c) should be compared with figure 5(c).

At a Reynolds number of 550,000 the damping-in-pitch coefficient became positive at low oscillation amplitudes for Mach numbers greater than 0.85. At a Mach number of 0.90 oscillations built up to a steady-state amplitude of somewhat less than 2° with no external torque being supplied by the oscillator, and increasing the Mach number increased the

steady-state amplitude of the undamped oscillations. This unexpected variation of damping-in-pitch coefficient with Mach number and oscillation amplitude was repeatable and little affected by frequency. It was observed at zero angle of attack and at high subsonic Mach numbers but was not apparent at the other angles of attack at which tests were conducted.

There is a superficial similarity in the variation of damping-in-pitch coefficient with oscillation amplitude at the two Reynolds numbers after the damping becomes unstable. However, aside from the difference in Mach number at which instability was encountered in each case, there was also a difference in the character of the oscillations. At the lower Reynolds number the oscillations were smooth and no difficulty was experienced in maintaining a constant amplitude, whereas the instability at the higher Reynolds number was nearly always accompanied by transient aerodynamic disturbances and sudden variations in steady-state amplitude.

The application of roughness at the wing leading edge (fig. 10) resulted in a variation of damping-in-pitch coefficient with oscillation amplitude at a Reynolds number of 550,000 which was similar to that measured at a higher Reynolds number (fig. 5(a)). In view of this it appears that the instability which occurred at low Reynolds numbers and high Mach numbers was caused, at least partly, by the interaction of a shock wave with a laminar boundary layer, and that increased turbulence in the boundary layer in this case increased the Mach number at which instability was encountered. Further study of this phenomena is desirable particularly for Reynolds numbers higher than were possible in this test.

At low Mach numbers, the result of increasing the Reynolds number to 6,000,000 was that variations in the damping-in-pitch coefficient with oscillation amplitude and with angle of attack became less (fig. 11). At zero angle of attack there was practically no effect of scale for Reynolds numbers between 1,250,000 and 6,000,000 at a Mach number of 0.23.

Effects of Angle of Attack

Figures 12, 13, and 14 summarize a large amount of data on effects of a variation in angle of attack. The points shown were taken for an amplitude of 2° from faired curves of the variation of damping-in-pitch coefficient with oscillation amplitude. It is apparent that Reynolds number is a significant variable in considering the effect of angle of attack (fig. 12) and that increasing the Reynolds number above 1,250,000 resulted in smaller variations of damping-in-pitch coefficient with angle of attack. At high Mach numbers and Reynolds numbers of 550,000 and 1,250,000 (figs. 13 and 14), the damping-in-pitch in most cases increased from its value at zero angle of attack to a higher value at

an angle of attack of 4°. As the angle of attack was increased beyond 4°, the stability gradually decreased. During the test it was noted that this decrease in stability was also accompanied by intermittent aerodynamic disturbances which increased in severity as the angle of attack was increased. The dashed curves in figures 12, 13, and 14 indicate approximately where the oscillation was completely dominated by these transient disturbances.

Effects of Frequency

The variation of damping-in-pitch coefficient with reduced frequency presented in figure 15 was obtained from the data of figure 5. The reduced frequency is a dimensionless term which relates the oscillation frequency to the forward velocity and the length of the mean aerodynamic chord. Geometrically similar aircraft or models oscillating in an air stream at the same Reynolds number and Mach number would be acted on by the same force and moment coefficients if the reduced frequencies were the same, even though the oscillation frequencies were different.

A general trend in the variation of damping coefficient with reduced frequency is not apparent in figure 15. The data taken at an oscillation frequency of 19 cps are largely responsible for the irregular depression in each cross-plot curve at a different reduced frequency, and the possibility exists that some resonant condition in the test apparatus is responsible for this. Resonance effects of the model support were investigated at 15 cps (fig. 16) and were found to be negligible within experimental accuracy. It would be expected that resonance effects at 19 cps would manifest themselves to some extent at this lower frequency. Resonance of some part of the model structure would be expected to appear in the wind-off damping but no effects are apparent in figure 4. The data for 19 cps are repeatable (fig. 5(c)) and consistent with other data at the same frequency (figs. 6 and 12). No explanation can be given for the type of variation shown in figure 15 although indications are that aerodynamic effects are not responsible.

In figure 7 it is shown that for Mach numbers above 0.90 an increase in frequency resulted in a less drastic variation of damping in pitch with Mach number. At a frequency of 27 cps the damping-in-pitch coefficient was negative through the entire Mach number range.

Effects of Pitching Axis Position

A rearward movement of the pitching axis from 0.35 $\bar{c}$ to 0.45 $\bar{c}$ is shown to result in slightly more negative values of damping-in-pitch

coefficient for Mach numbers above 0.60 (fig. 17). For Mach numbers below 0.60 there appears to be no significant change in the damping-in-pitch coefficient for the range of parameters at which tests were conducted.

SUMMARY OF RESULTS

Results of an experimental investigation of the single-degree-of-freedom damping in pitch of a model triangular wing and body combination at subsonic Mach numbers have been summarized as follows:

1. At a Reynolds number of 1,250,000 and an angle of attack of zero, the damping-in-pitch coefficient became positive for Mach numbers above approximately 0.94 for all frequencies except the highest at which tests were conducted.

2. At a Reynolds number of 550,000 and an angle of attack of zero, the damping-in-pitch coefficient became positive, indicating instability, at low oscillation amplitudes for Mach numbers above 0.85, but the application of roughness to the wing increased the Mach number at which instability was encountered to 0.94.

3. A variation in angle of attack from 0° to 19° resulted in large variations in the damping-in-pitch coefficient at Reynolds numbers of 550,000 and 1,250,000. Limited data for Reynolds numbers of 3,000,000 and 6,000,000 indicated that these variations became less as the Reynolds number was increased.

4. A variation of oscillation amplitude was found in most cases to have a large effect on the damping in pitch for the high Mach numbers at which instability was encountered. At low Mach numbers, however, the damping-in-pitch coefficient was essentially independent of oscillation amplitude.

5. A general trend in the variation of damping coefficient with reduced frequency was not apparent for Mach numbers below 0.94, but for Mach numbers of about 0.94 an increase in frequency resulted in greater stability.

6. A movement of the pitching axis from 0.35 $\bar{c}$ to 0.45 $\bar{c}$ resulted in only minor changes in the damping-in-pitch coefficient.

Ames Aeronautical Laboratory
National Advisory Committee for Aeronautics
Moffett Field, California

[redacted]

REFERENCES

1. Tobak, Murray, Reese, David E., Jr., and Beam, Benjamin H.: Experimental Damping in Pitch of 45° Triangular Wings. NACA RM A50J26, 1950.

2. Aigrain, Pierre R., and Williams, Everard M.: Theory of Amplitude-Stabilized Oscillators. Proceedings of the IRE, vol. 36, no. 1, Jan. 1948.

3. Durand, William Frederick: Aerodynamic Theory. Vol. V., Julius Springer, Berlin, 1934. (CIT Reprint) p. 49.

4. Herriot, John G: Blockage Corrections for Three-Dimensional-Flow Closed-Throat Wind Tunnels With Consideration of the Effect of Compressibility. NACA Rep. 995, 1950. (Formerly NACA RM A7B28)

5. Runyan, Harry L., and Watkins, Charles E.: Considerations on the Effect of Wind-Tunnel Walls on the Oscillating Air Forces for Two-Dimensional Subsonic Compressible Flow. NACA TN 2552, 1951.

6. Lamb, Horace: Hydrodynamics, Sixth Edition, Dover Pub., New York, 1945, p. 527.

7. Heitmeyer, John C., and Stephenson, Jack D.: Lift, Drag, and Pitching Moment of Low-Aspect-Ratio Wings at Subsonic and Supersonic Speeds - Plane Triangular Wing of Aspect Ratio 4 With NACA 0005-63 Section. NACA RM A50K24, 1951.

TABLE I.- INDEX OF RESULTS

Figure number	$C_{m_q} + C_{m_{\dot{\alpha}}}$ presented vs	Mach number	Reynolds number	Angle of attack (deg)	Frequency (cps)	Pitching axis ($X_r/\bar{c}$)	Other variables
5	θ_{max}	0.23 to 0.95	1,250,000	0	11 to 27	0.35	---
6	↓	↓	↓	↓	19	0.40 and 0.45	---
7	M	↓	↓	↓	11 to 27	0.35	---
8	↓	↓	↓	↓	11	↓	comparison with reference 1
9	θ_{max}	0.10 to 0.95	550,000	↓	11 and 19	↓	---
10	↓	0.85 to 0.93	↓	↓	11	↓	surface roughness[1]
11	↓	0.23	1,250,000 to 6,000,000	0 to 12	11 and 19	↓	---
12	α_o	0.10 and 0.23	550,000 to 6,000,000	---	↓	↓	---
13	↓	0.80 to 0.94	550,000	---	↓	↓	---
14	↓	0.80 to 0.92	1,250,000	---	11	↓	---
15	$\frac{\omega\bar{c}}{2V}$	0.23 to 0.92	↓	0	---	↓	---
16	α_o and M	0.23 to 0.94	↓	---	15	↓	vibration characteristics of model support
17	M	↓	↓	0	19	0.35 to 0.45	---

[1]A spanwise strip of number 60 carborundum particles, approximately 30-percent particle density, was applied from the wing leading edge to the 0.04-chord point on both upper and lower surfaces.

[redacted]

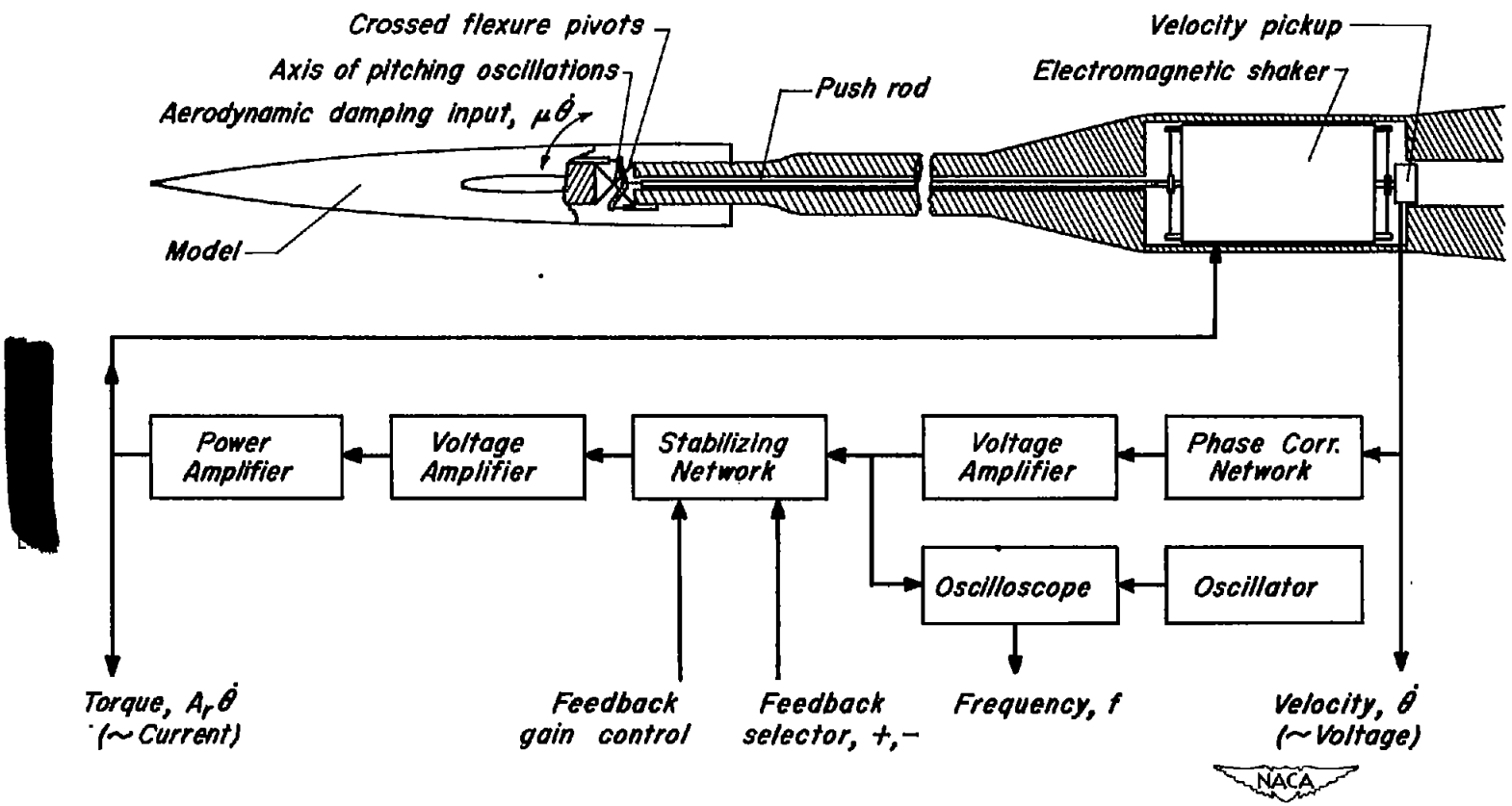

Figure 1.— Schematic sketch of the oscillator showing principal electronic components in block form.

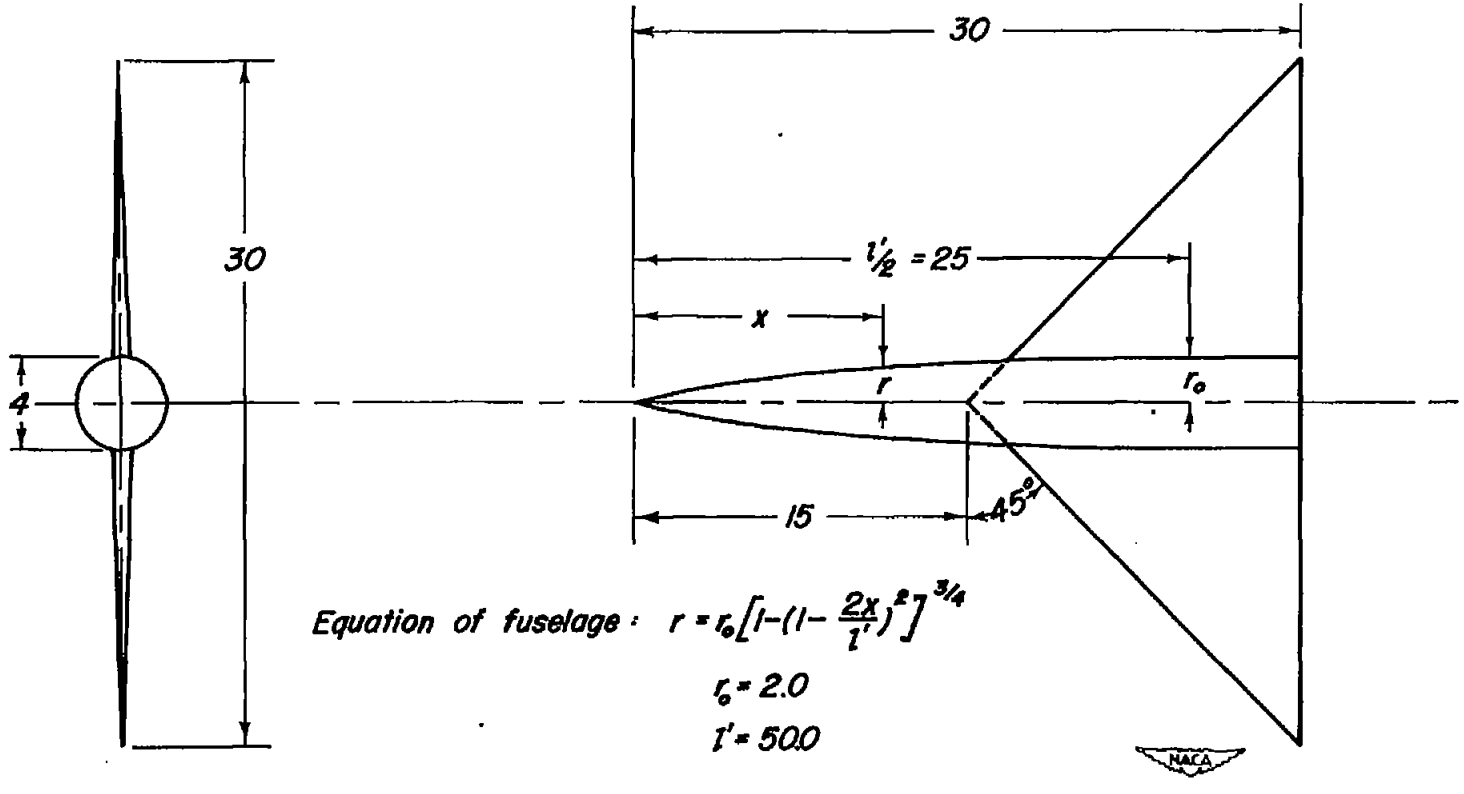

Note: All dimensions given in inches unless otherwise specified.

Figure 2.– Sketch of model.

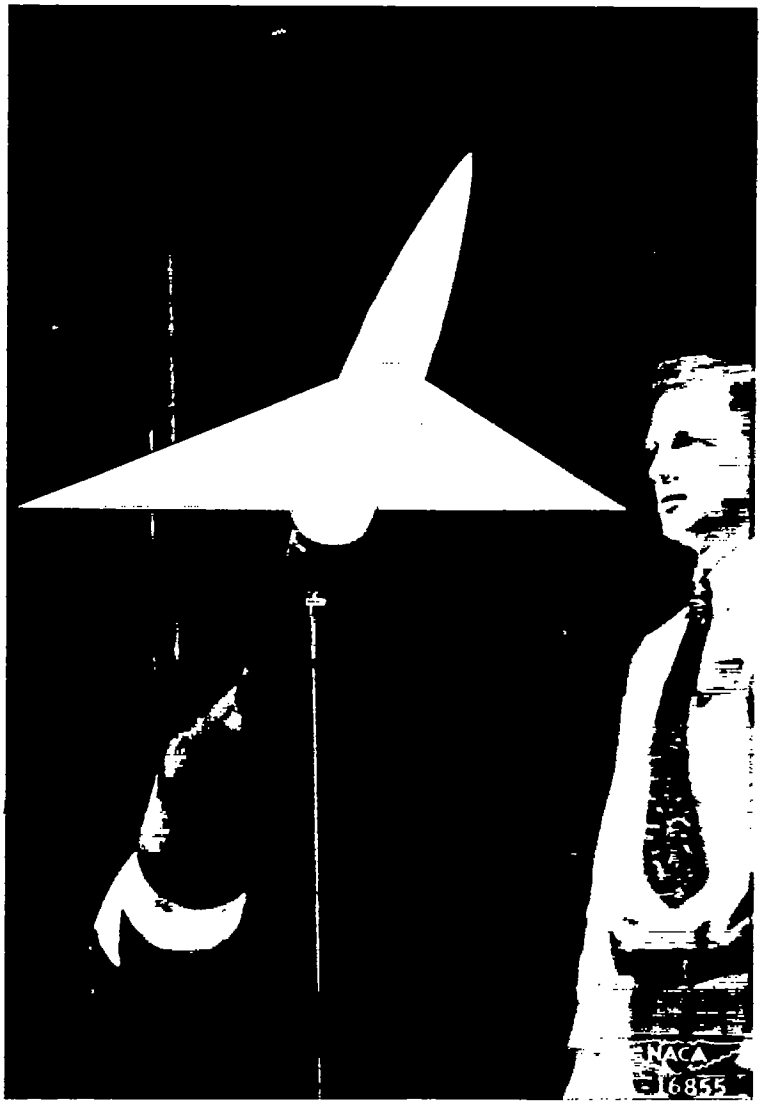

Figure 3.— Photograph of the model and model-support system. A 500-pound weight was suspended from the cable shown attached to the sting.

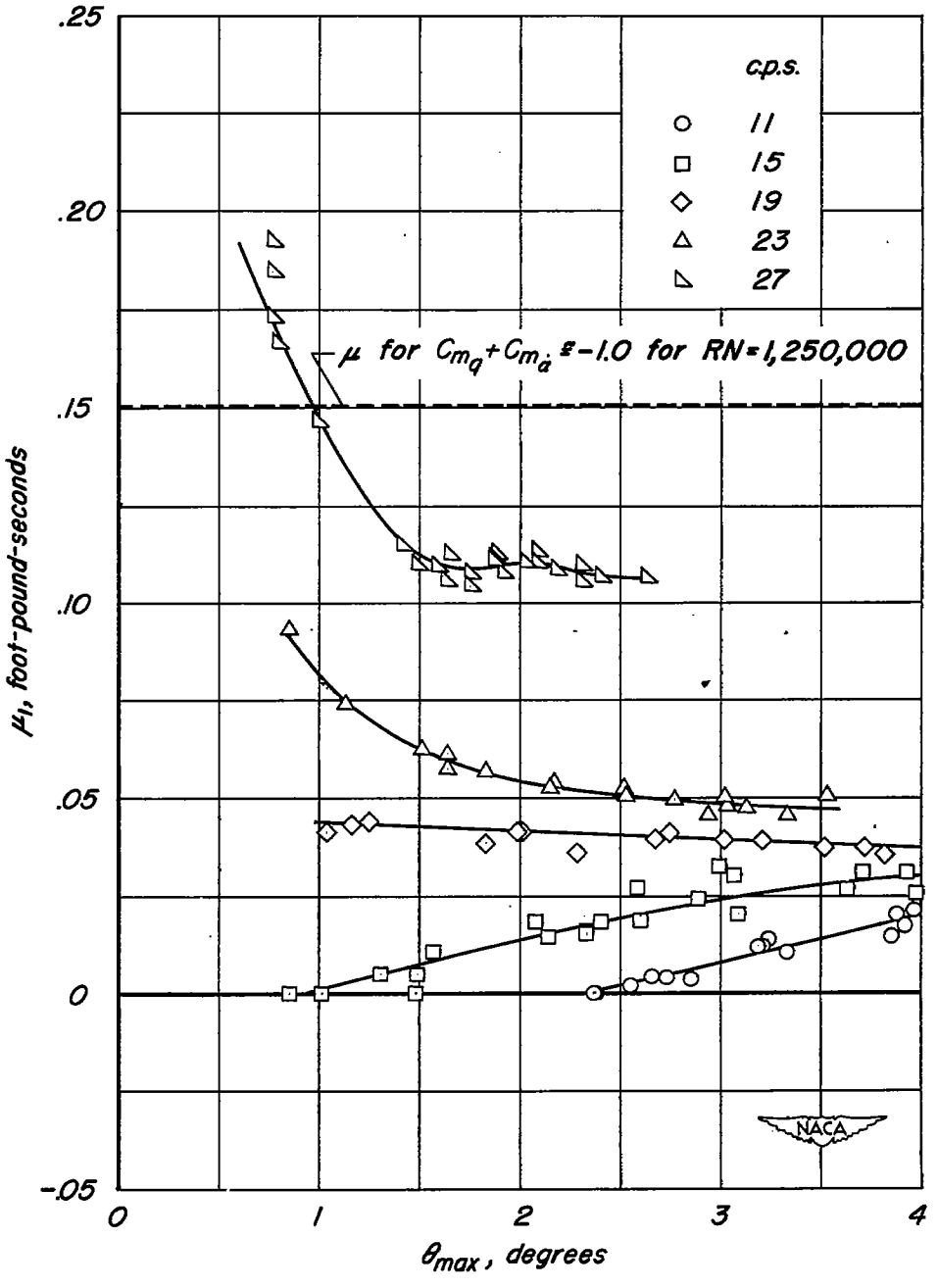

Figure 4. - The variation of the mechanical damping parameter with oscillation amplitude; $\frac{x_r}{c}$, 0.35.

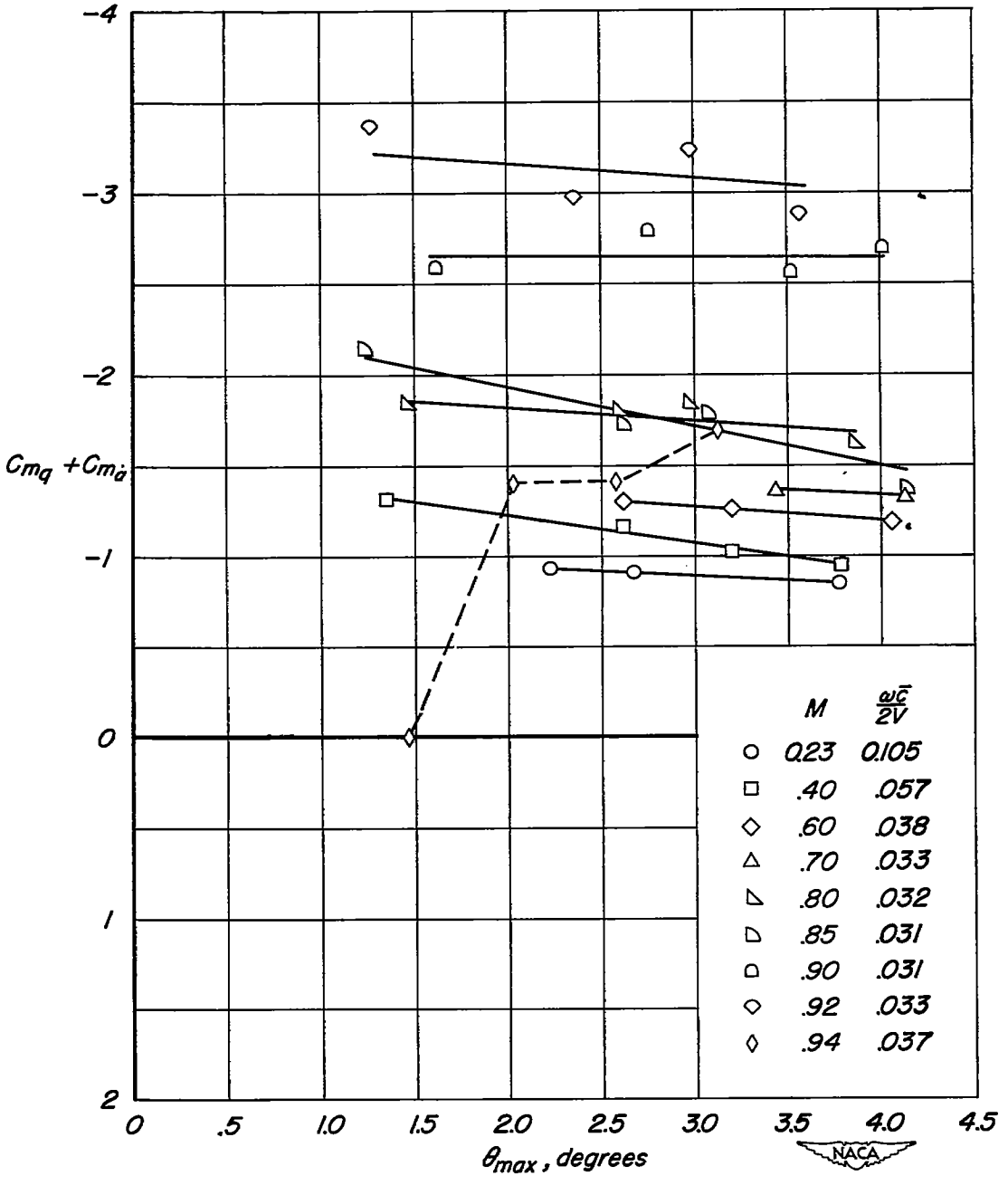

(a) f, 11 cps approx.

Figure 5.- The variation of damping-in-pitch coefficient with oscillation amplitude at zero angle of attack; $\frac{x_r}{\bar{c}}$, 0.35; RN, 1,250,000.

[redacted]

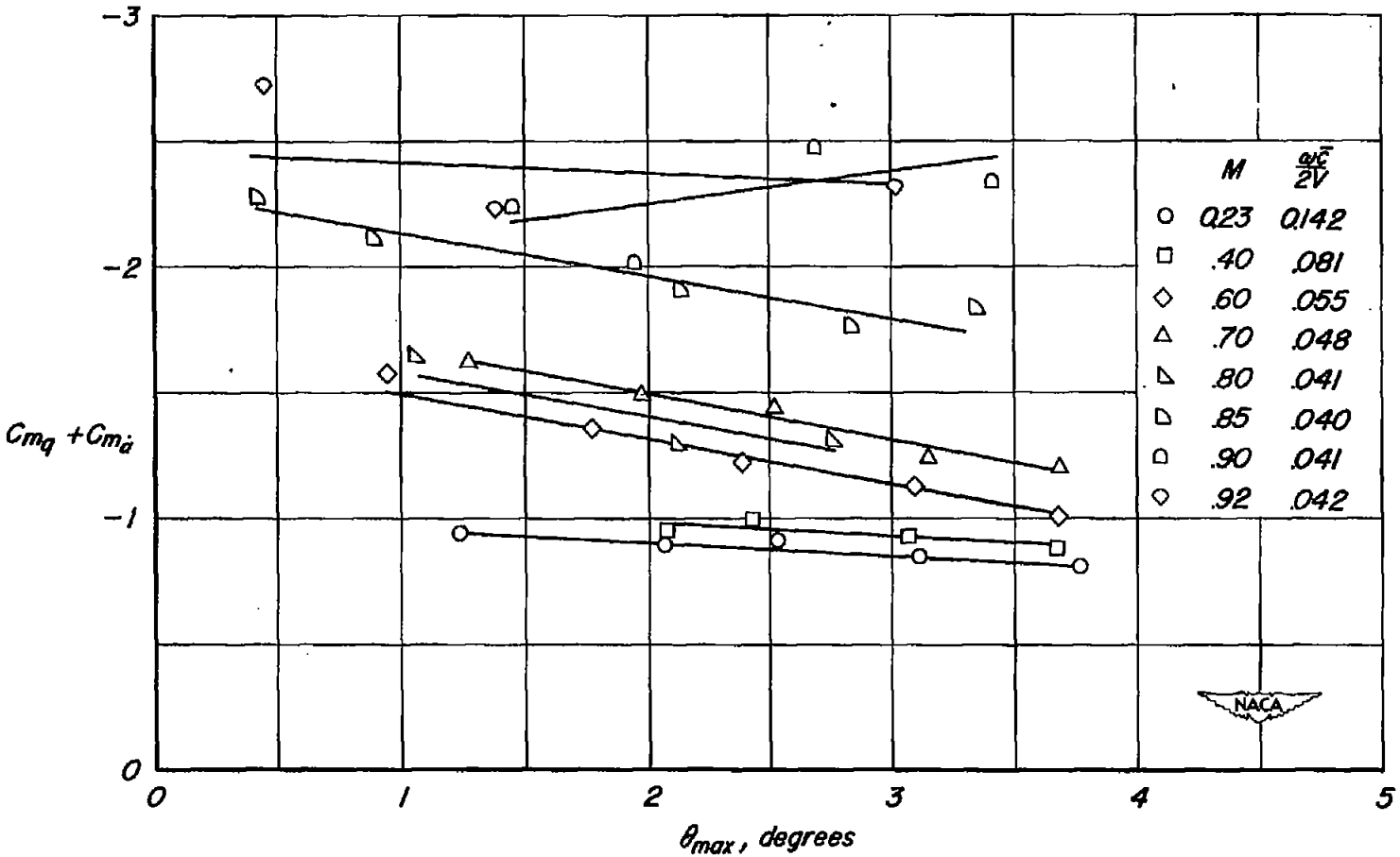

(b) f , 14 cps approx.

Figure 5.–Continued.

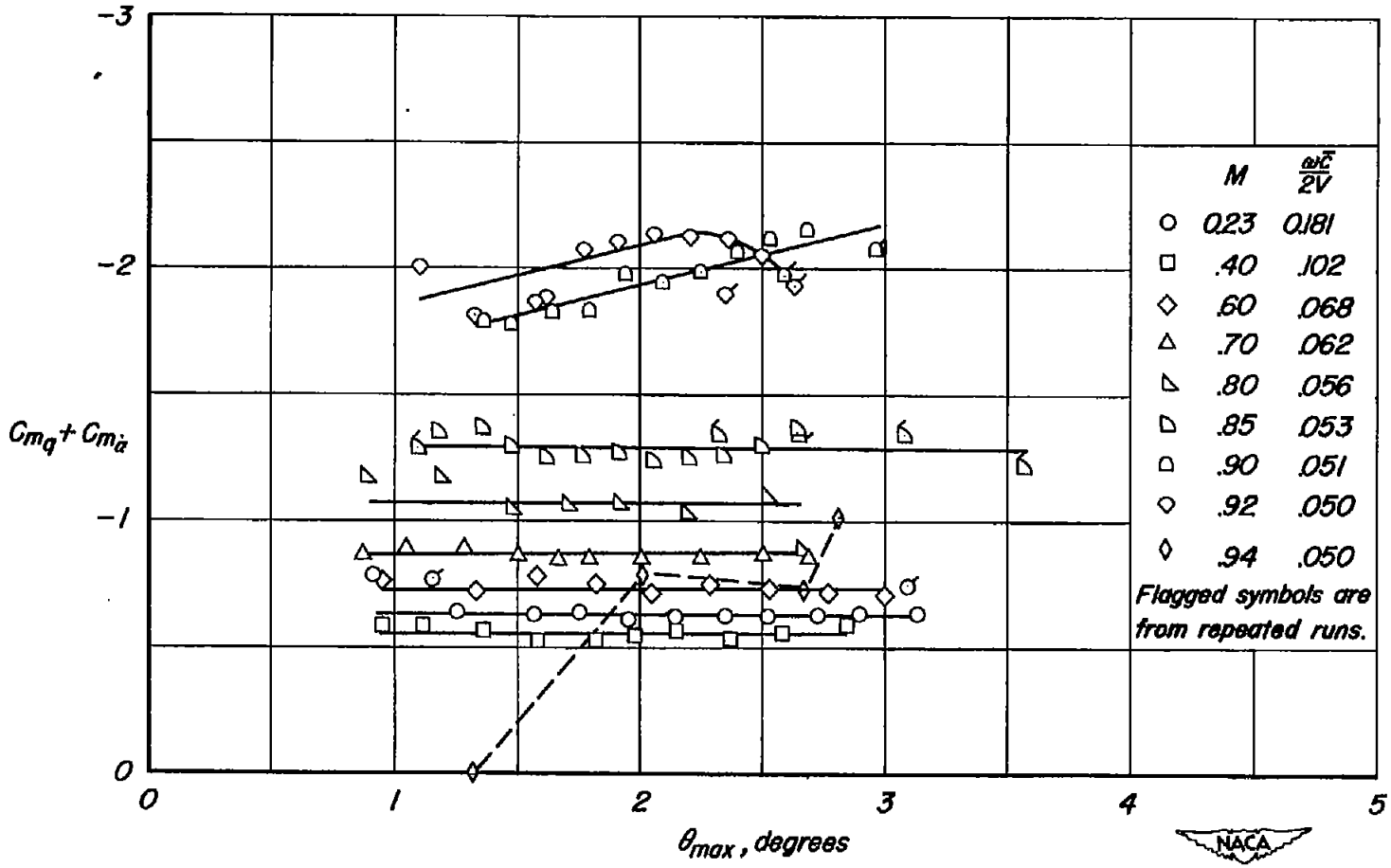

(c) f , 19 cps approx.

Figure 5.—Continued.

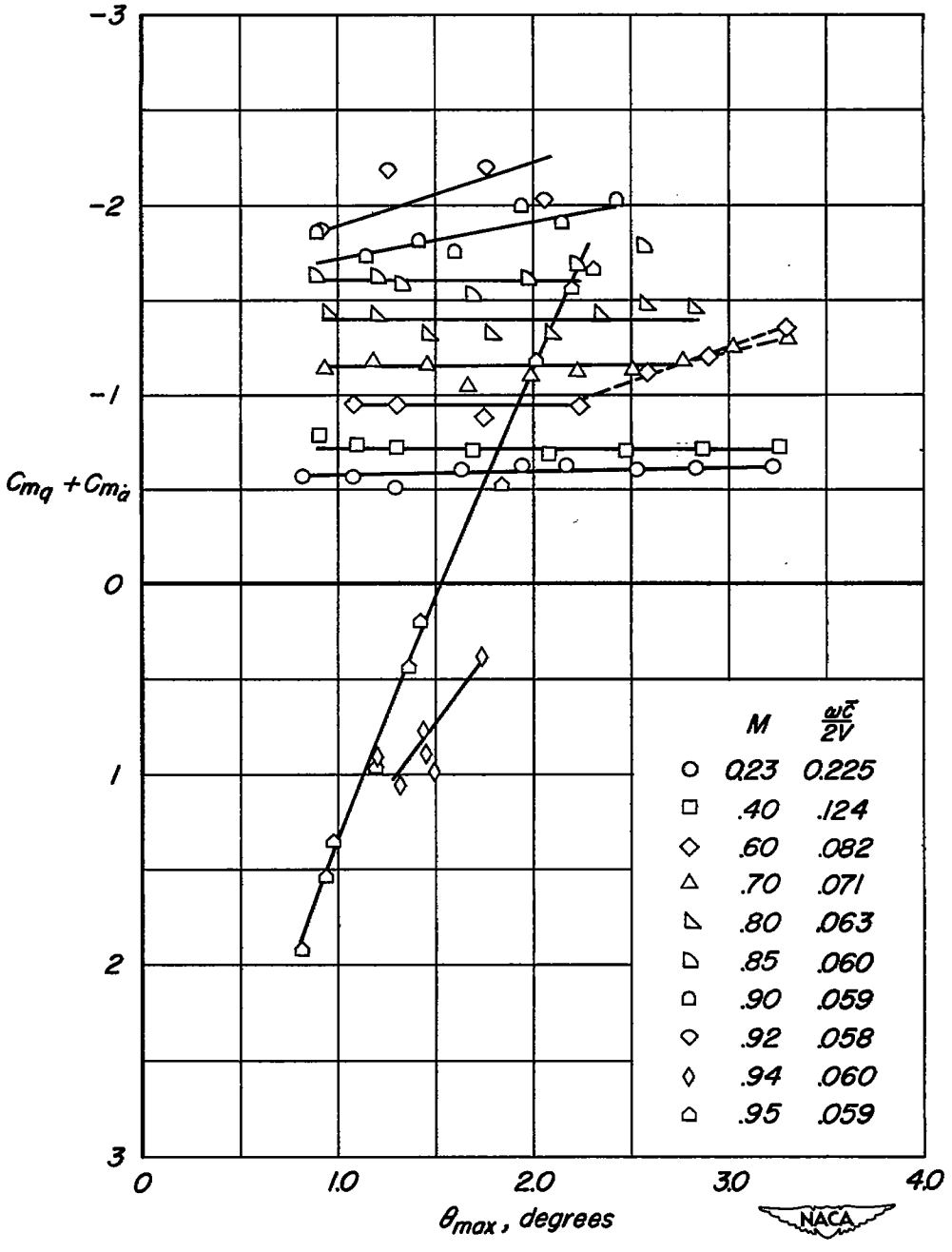

(d) f, 23 cps approx.

Figure 5.–Continued.

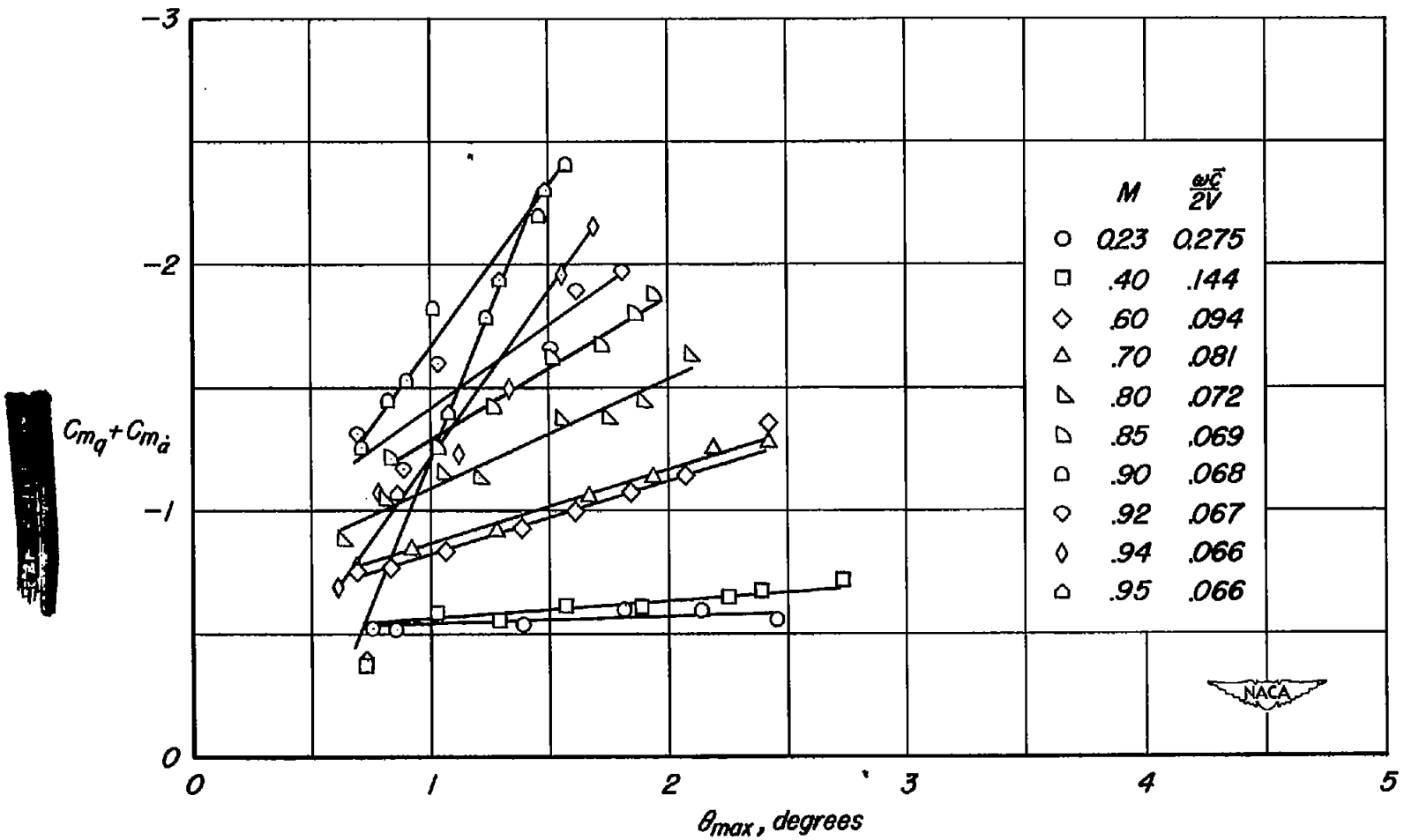

(e) f, 27 cps approx.

Figure 5.–Concluded.

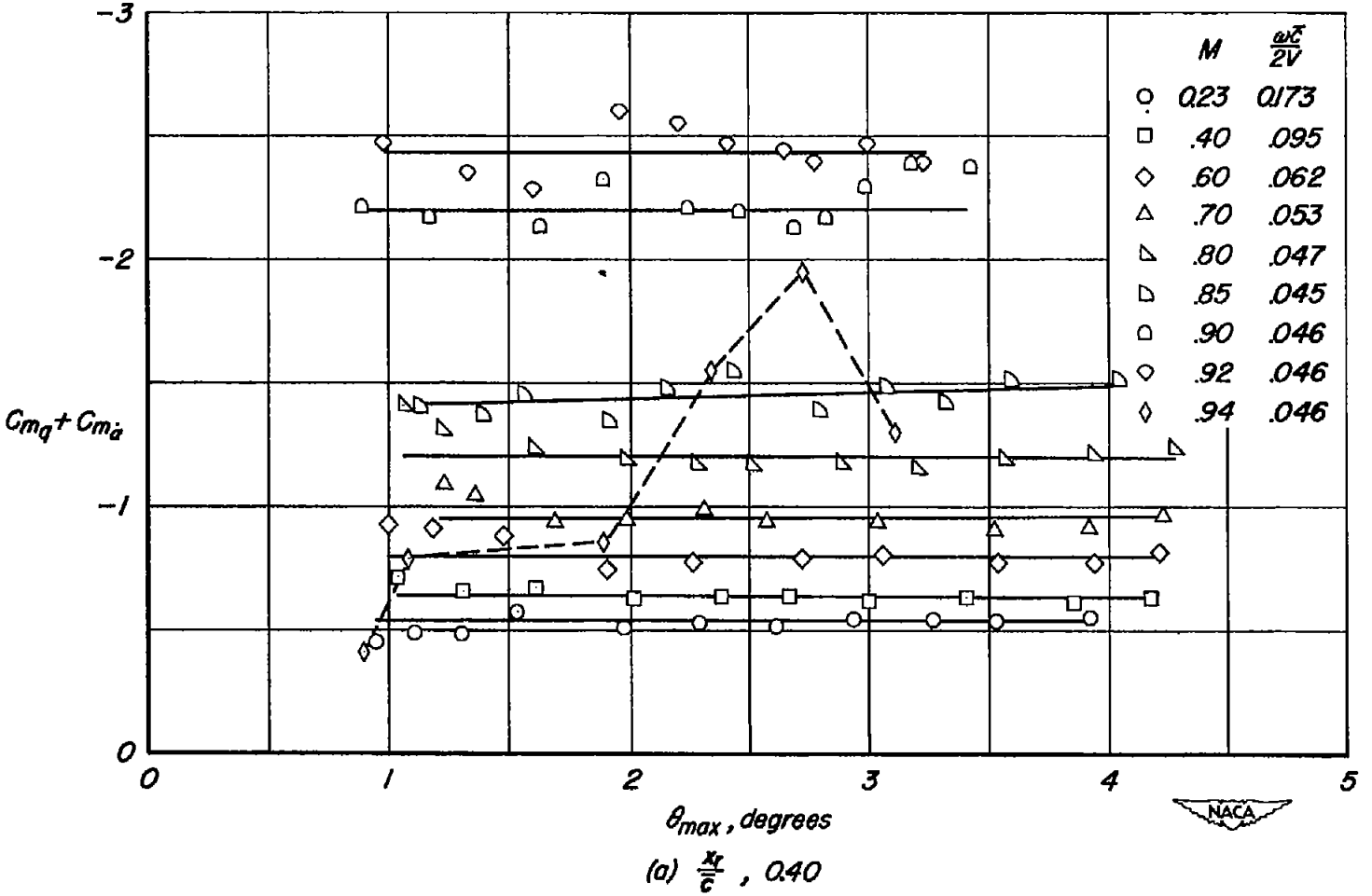

(a) $\frac{x_f}{c}$, 0.40

Figure 6.– The variation of damping-in-pitch coefficient with oscillation amplitude at zero angle of attack; f, 19 cps approx.; RN, 1,250,000.

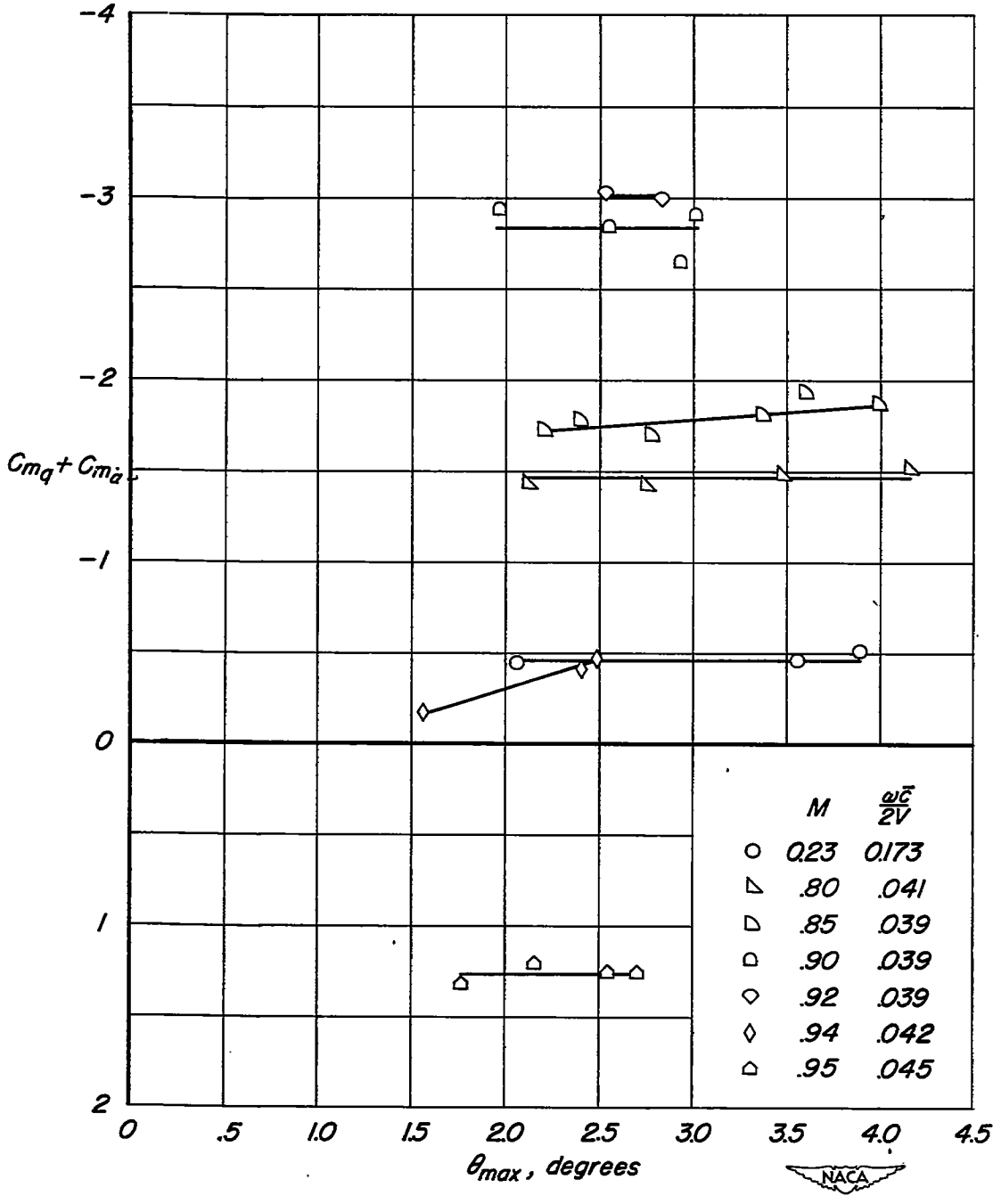

(b) $\frac{x_r}{c}$, 0.45

Figure 6.—Concluded.

[redacted]

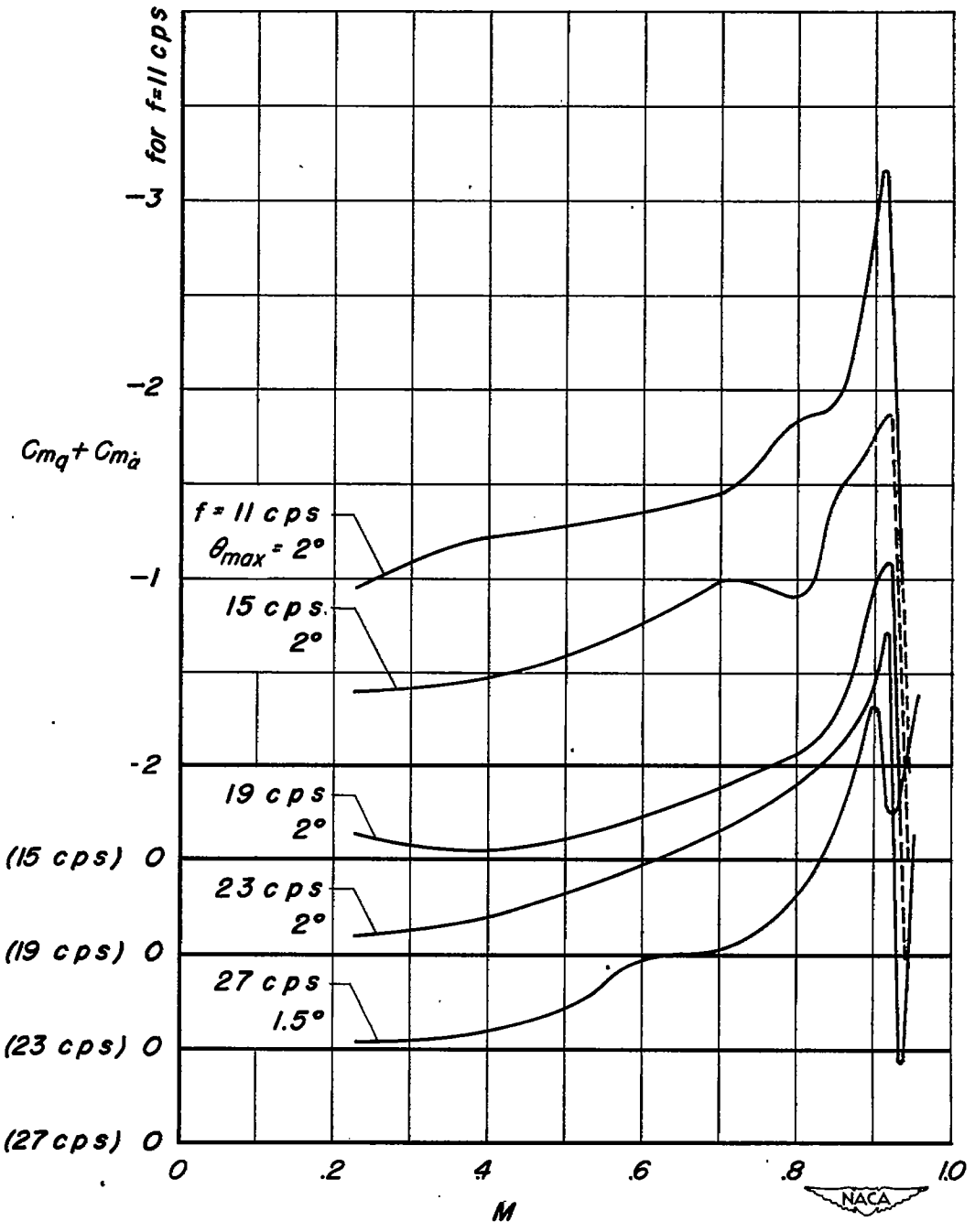

Figure 7.–The variation of damping-in-pitch coefficient with Mach number; $\frac{x_r}{c}$, 0.35 ; α_o, 0°; RN 1,250,000.

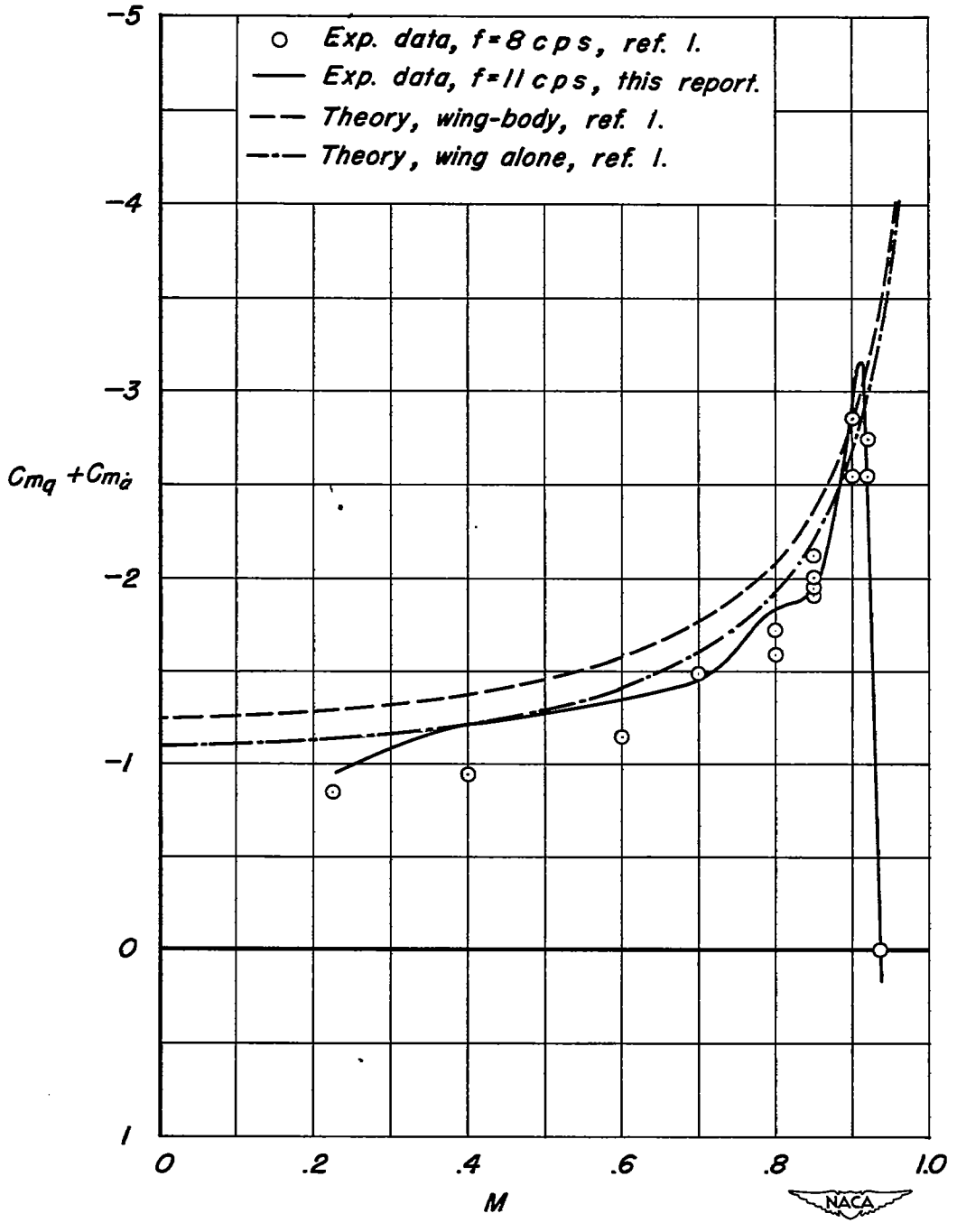

Figure 8.–A comparison of data of this report with data and theory from reference 1; a_o, 0°; $\frac{x_r}{c}$, 0.35; RN, 1,250,000.

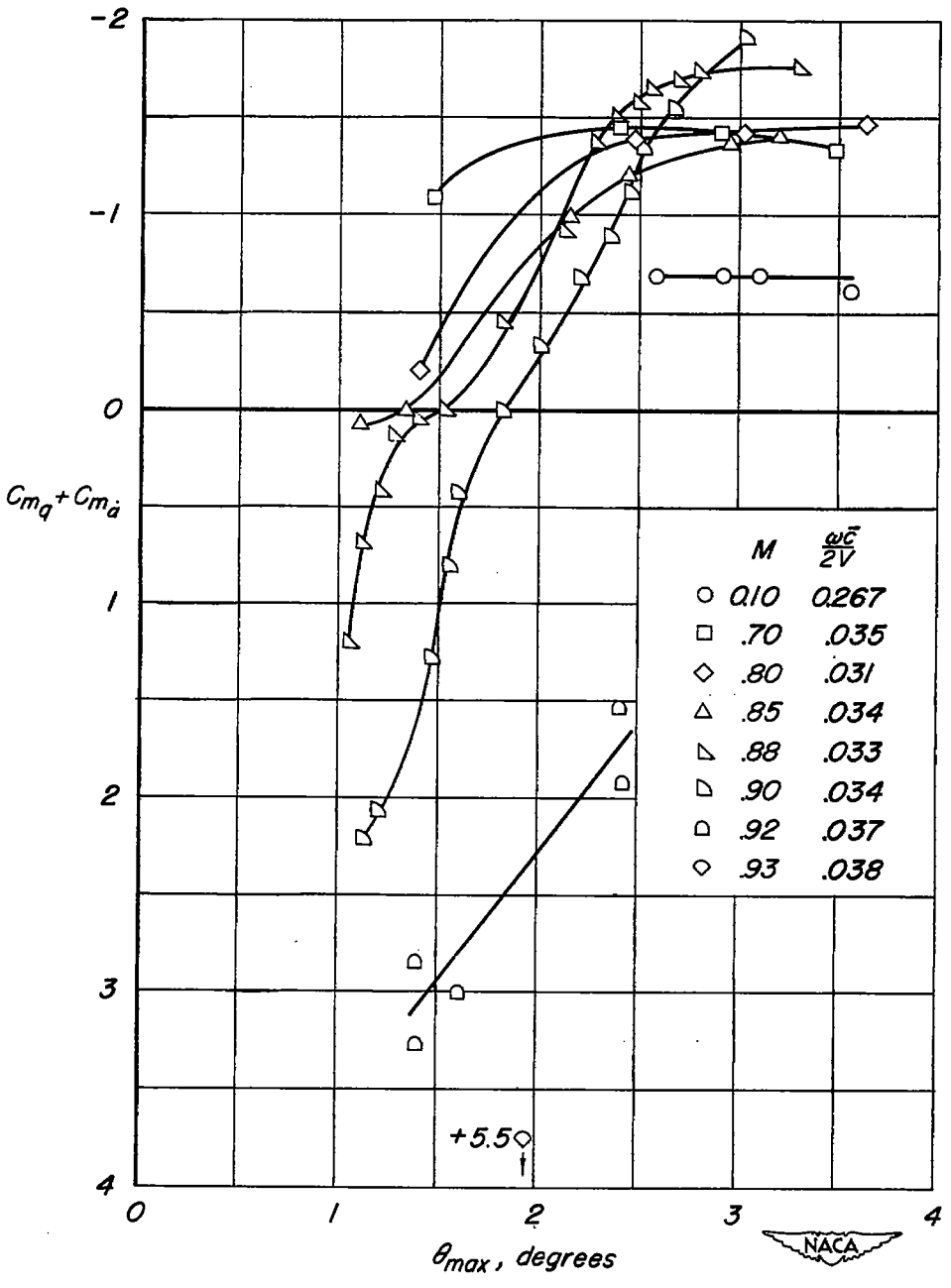

(a) f, 11 cps approx.

Figure 9.- The variation of damping-in-pitch coefficient with oscillation amplitude at zero angle of attack; $\frac{x_r}{c}$, 0.35; RN, 550,000.

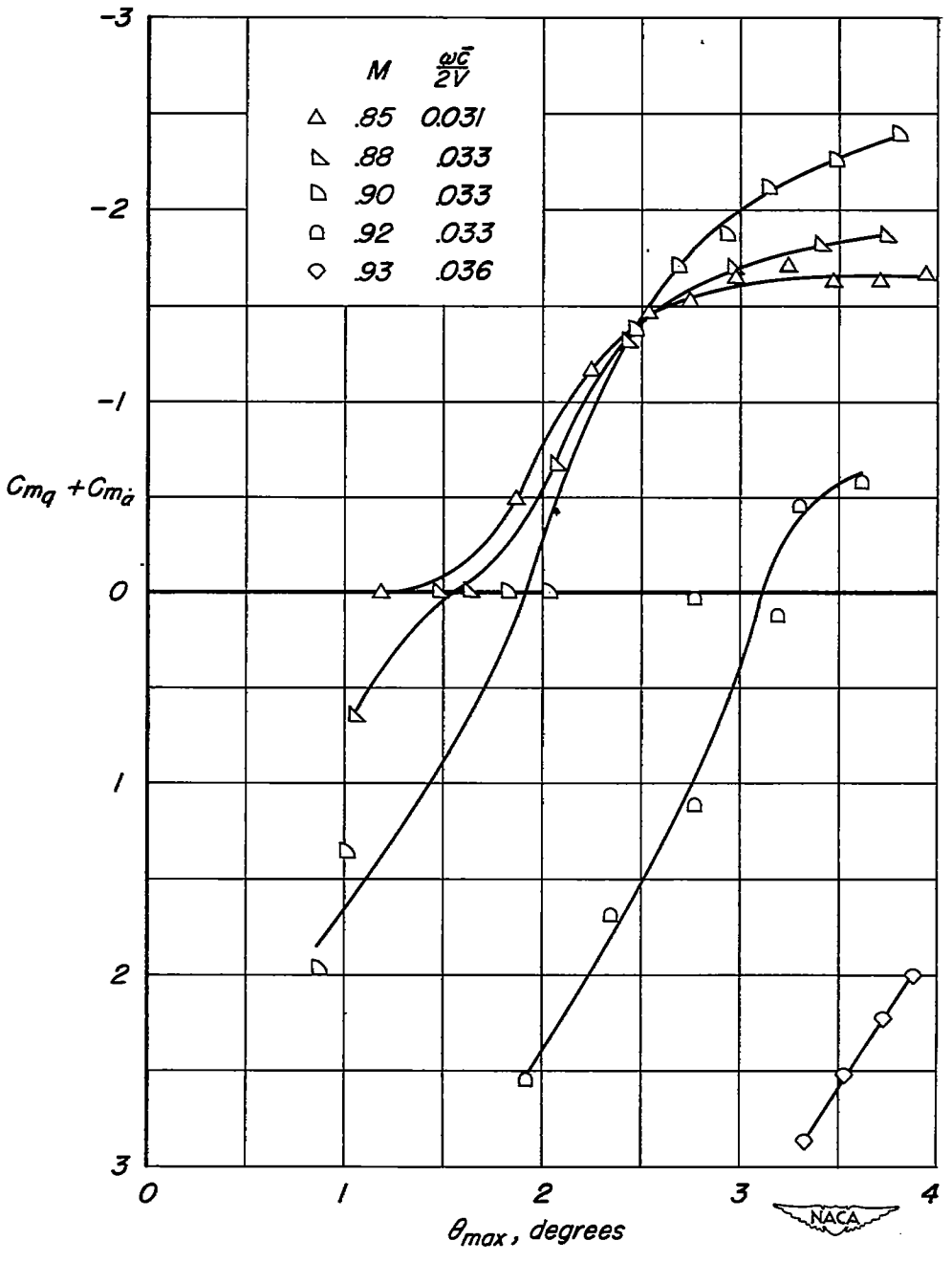

(b) f, 11 cps approx.

Figure 9.—Continued.

[redacted]

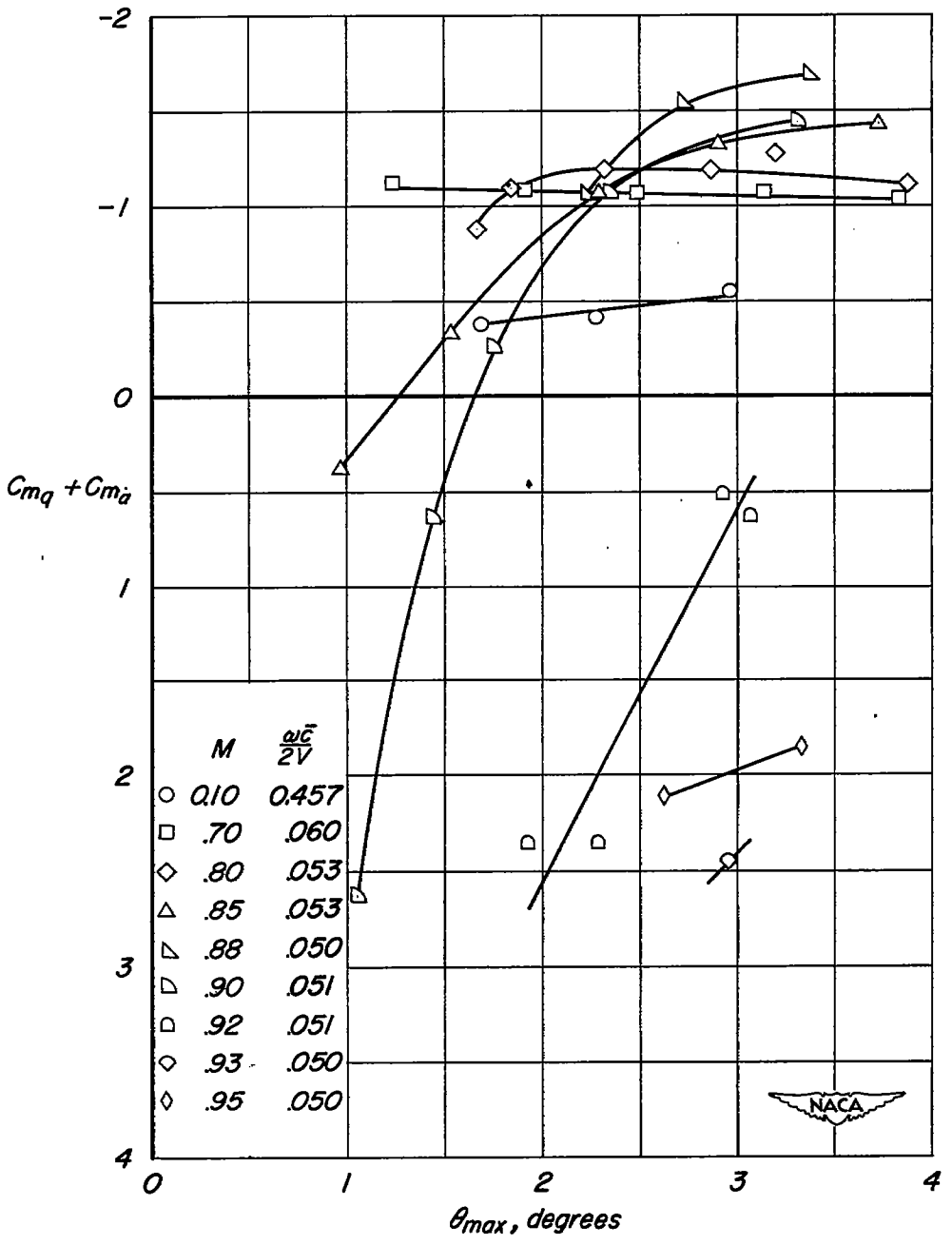

(c) f, 19 cps approx.

Figure 9.—Concluded.

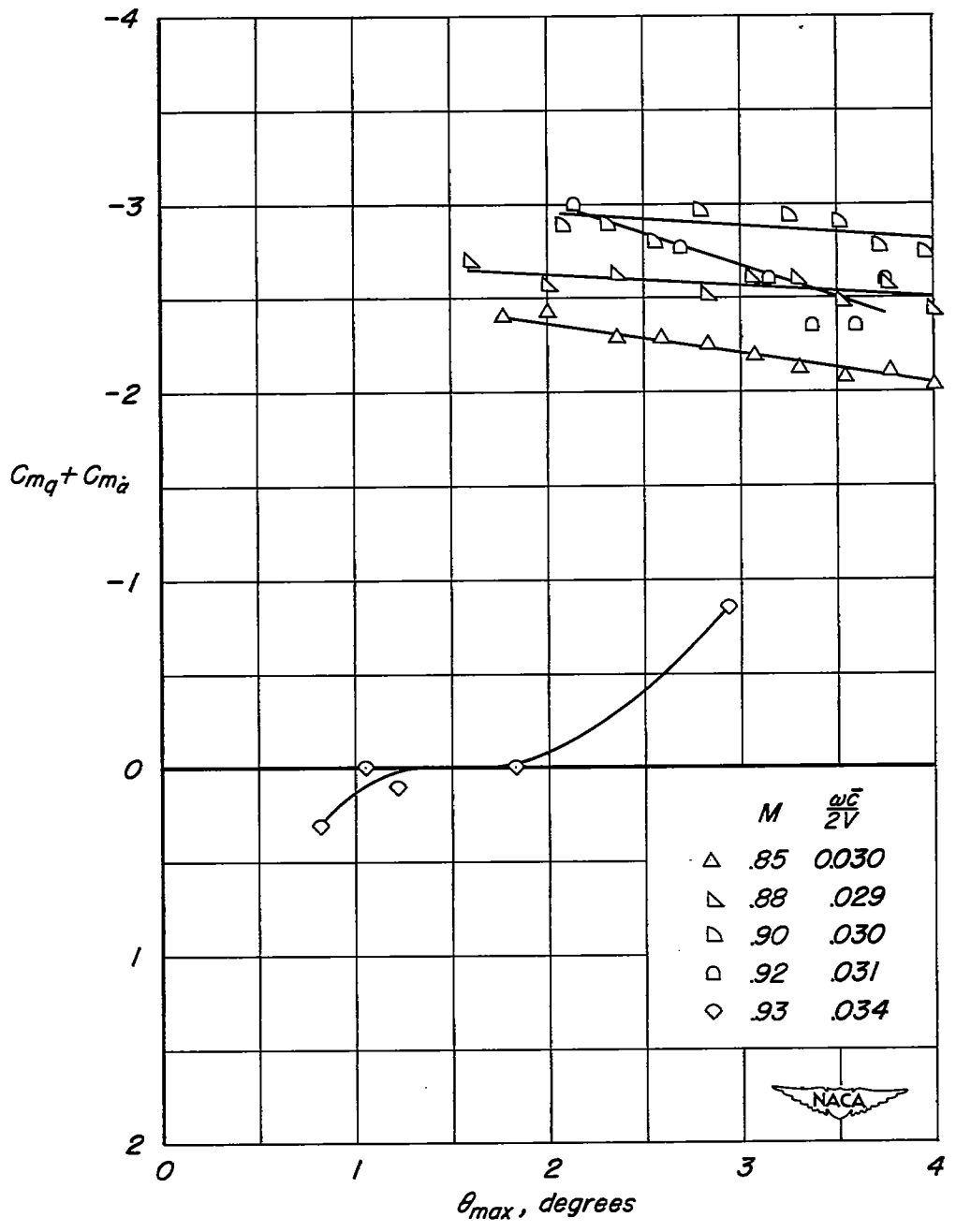

Figure 10.– The variation of damping-in-pitch coefficient with oscillation amplitude at zero angle of attack with roughness at the wing leading edge; $\frac{x_r}{c}$, 0.35; f, 11 cps approx.; RN, 550,000.

[redacted]

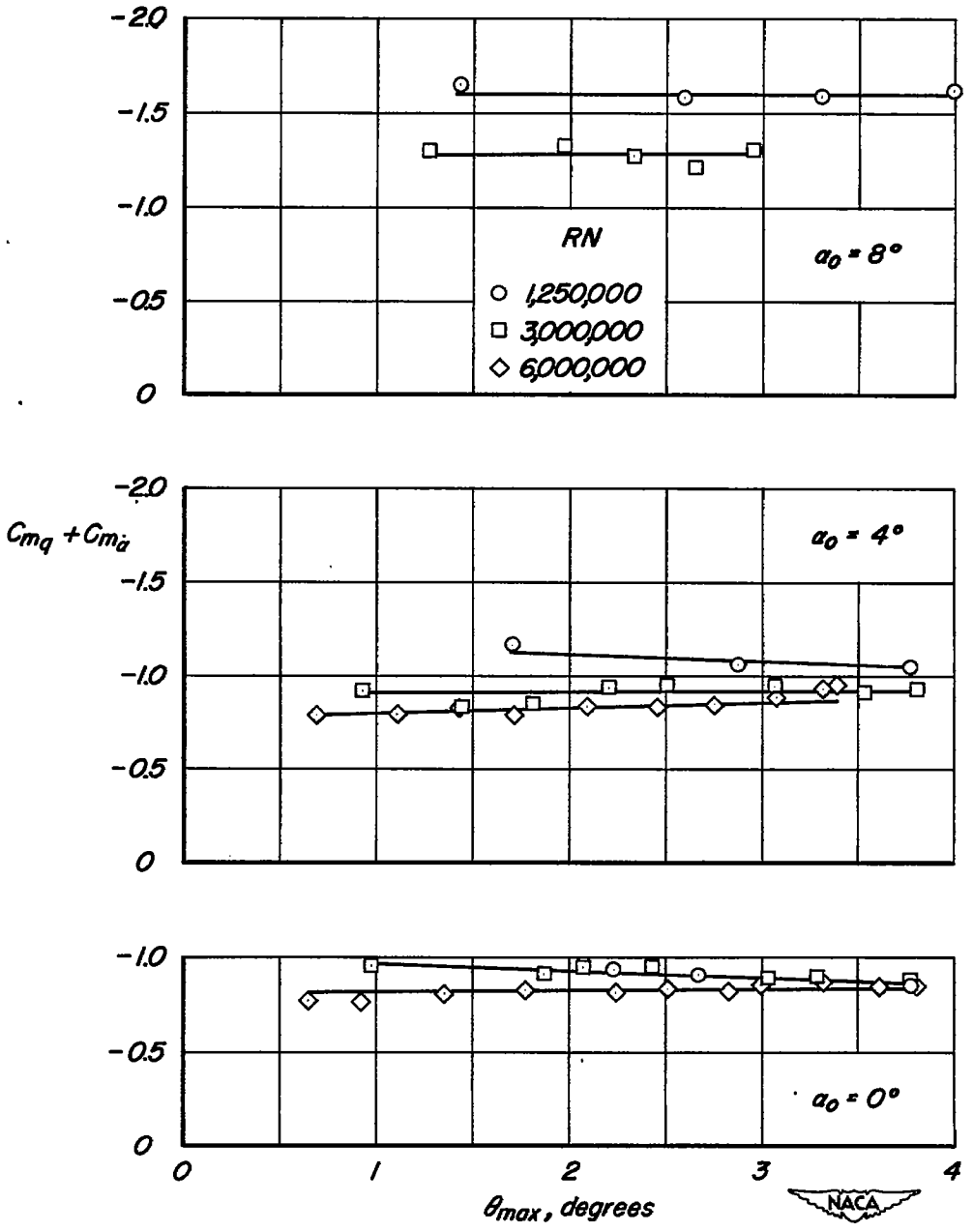

(a) f, 11 cps approx.

Figure 11.- The variation of damping-in-pitch coefficient with oscillation amplitude for three Reynolds numbers; M, 0.23; $\frac{x_r}{c}$, 0.35.

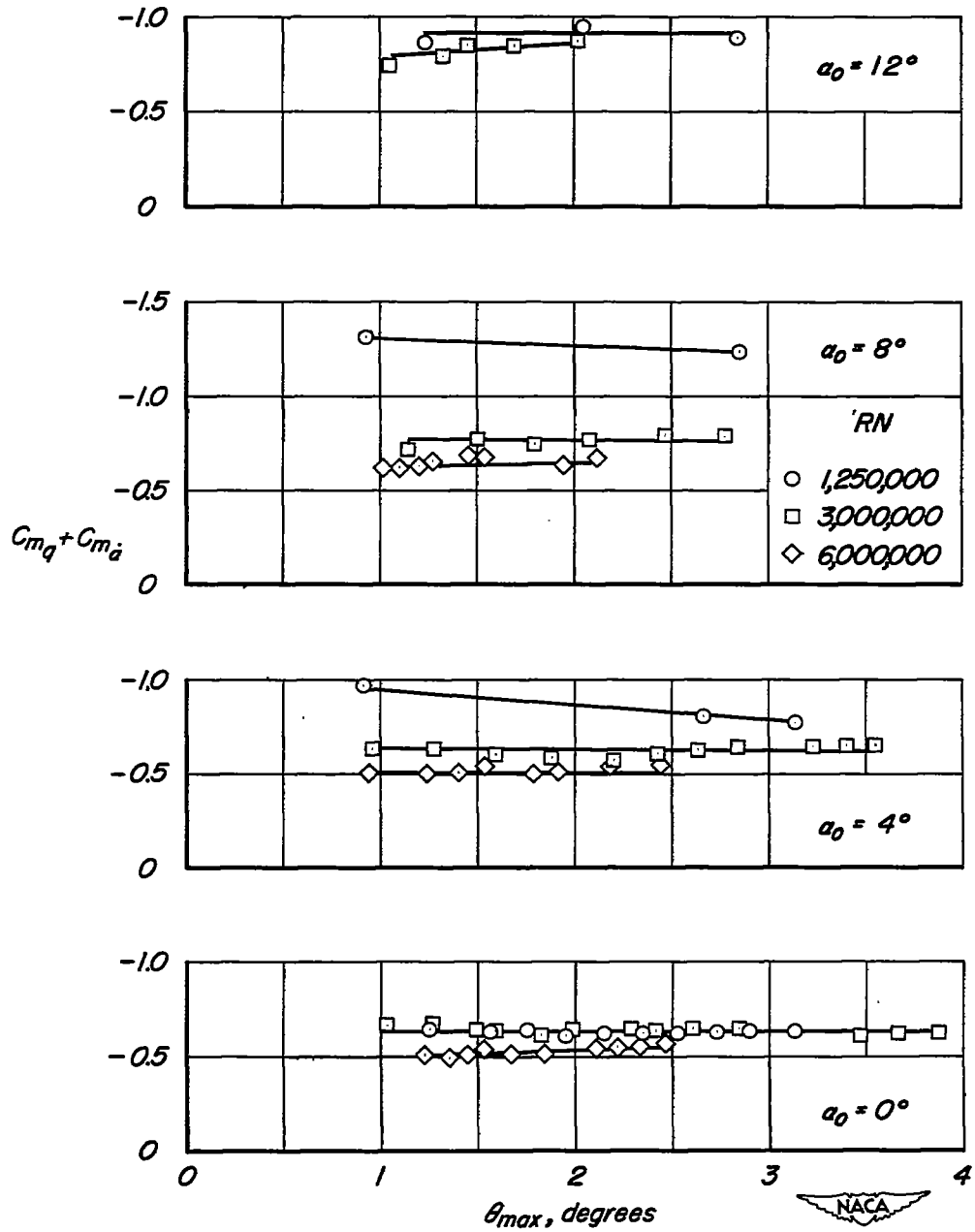

(b) f , 19 cps approx.

Figure 11.–Concluded.

[redacted]

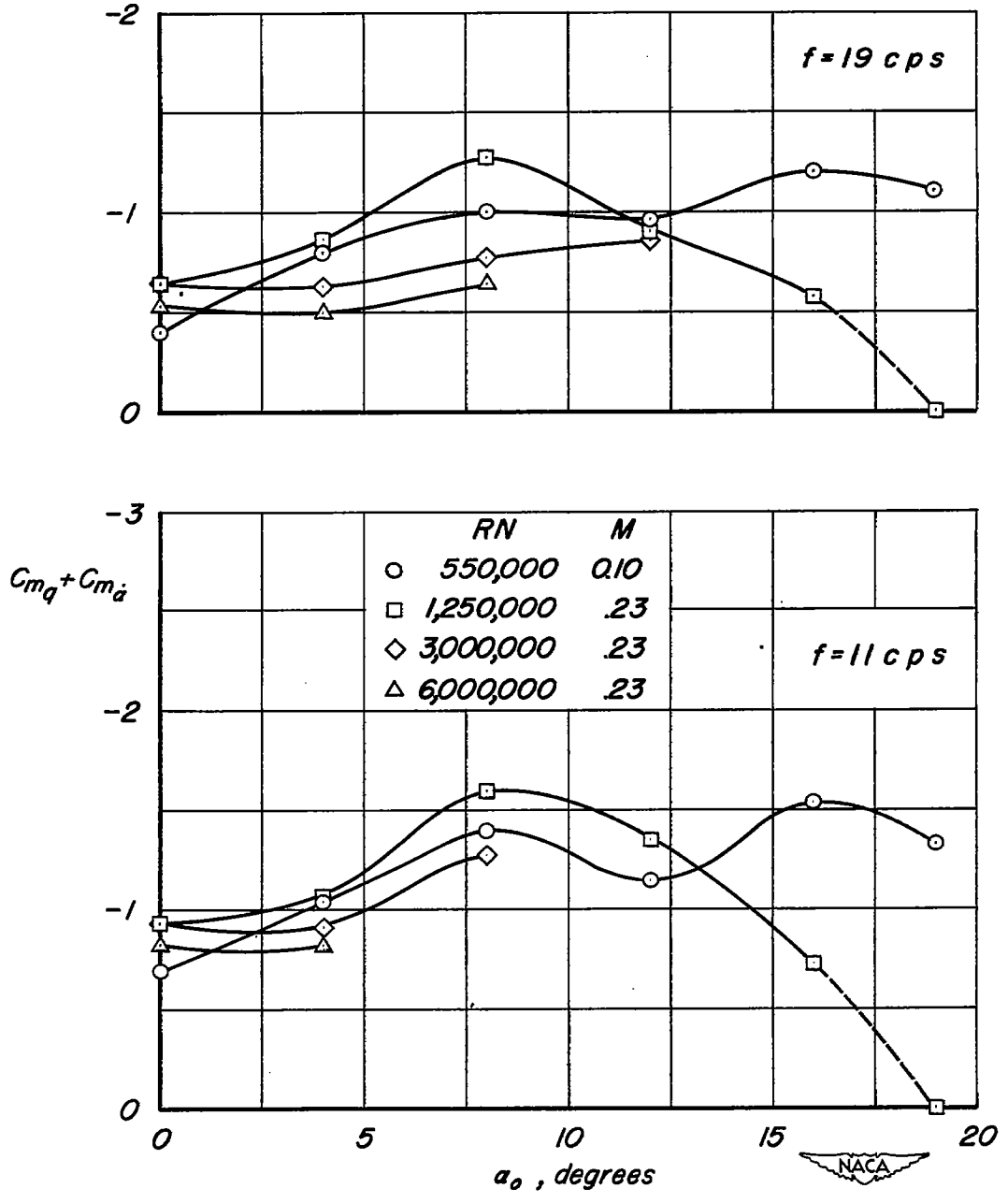

Figure 12.–The variation of damping-in-pitch coefficient with angle of attack for an oscillation amplitude of 2°; $\frac{x_r}{c}$, 0.35.

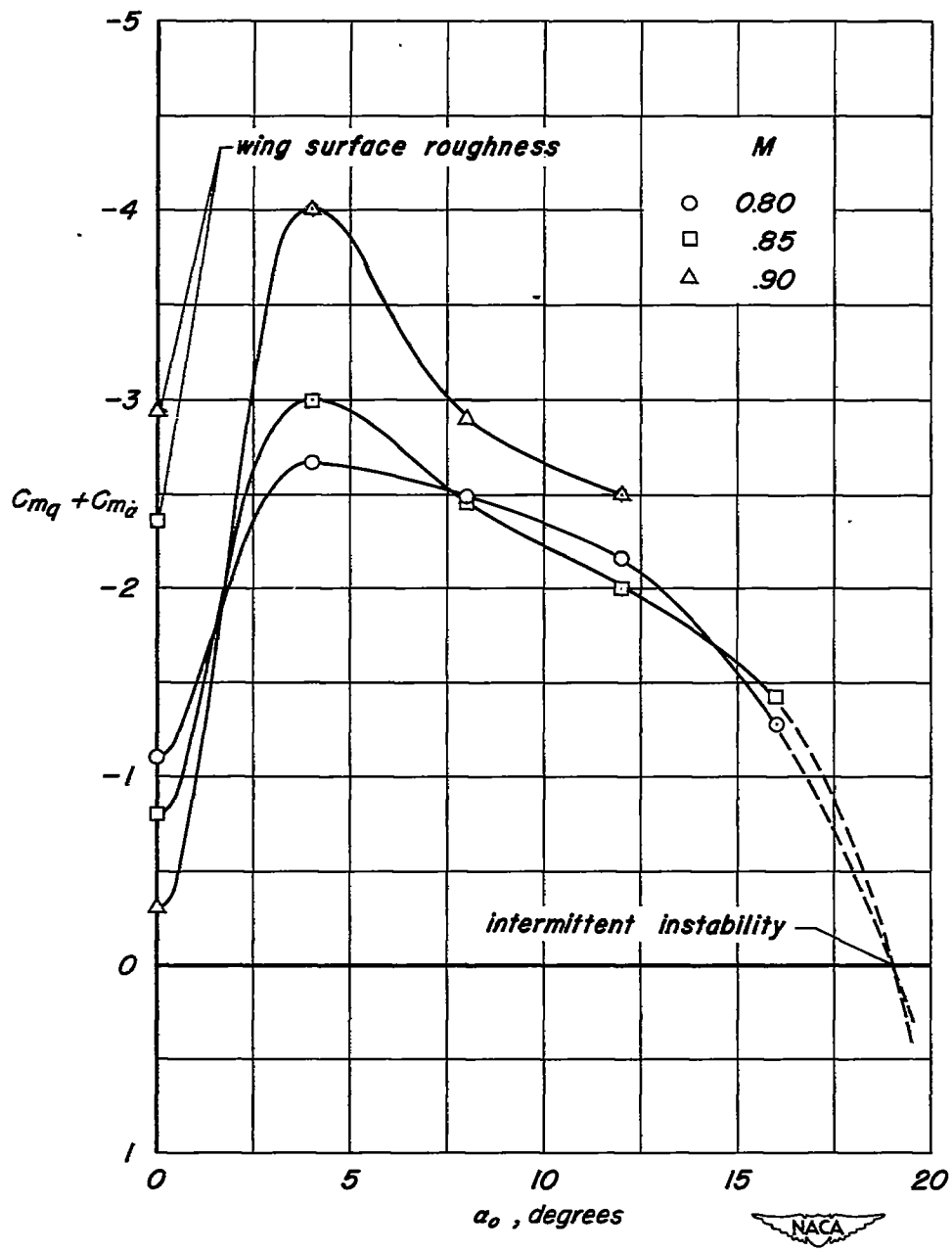

(a) f, 11 cps approx.

Figure 13.–The variation of damping-in-pitch coefficient with angle of attack for an oscillation amplitude of 2°; $\frac{x_r}{c}$, 0.35; RN, 550,000.

[redacted]

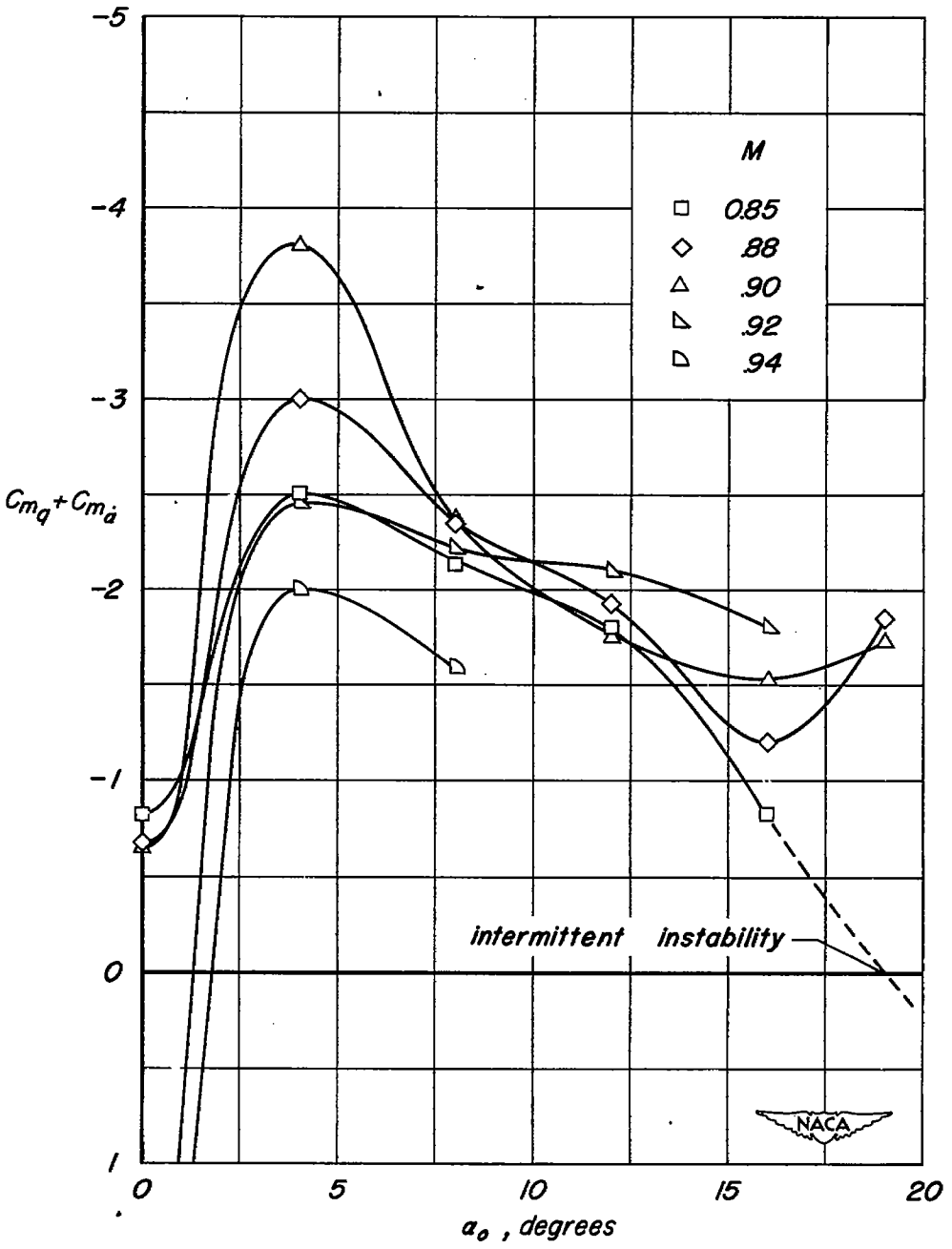

(b) f, 19 cps approx.

Figure 13.–Concluded.

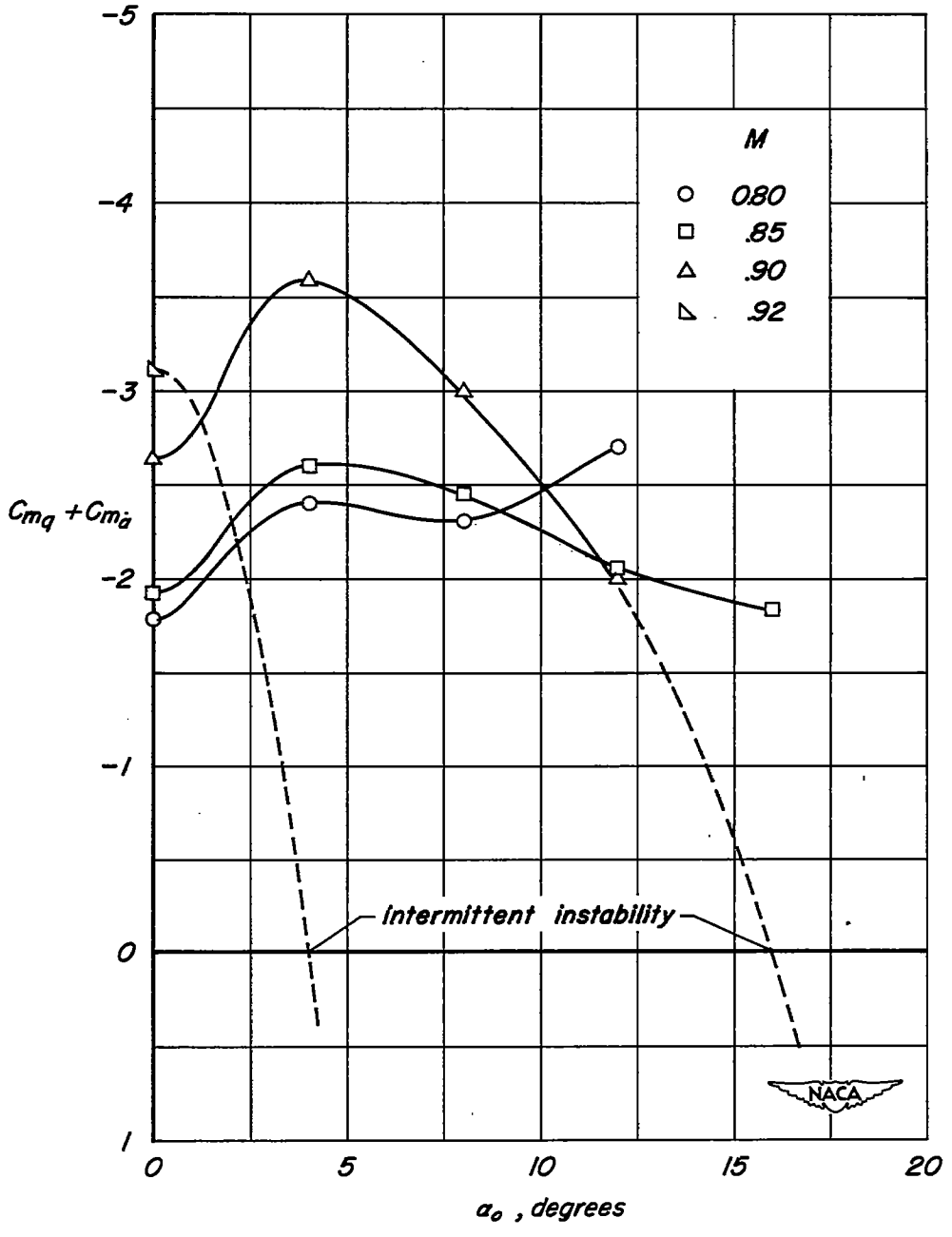

Figure 14.—The variation of damping-in-pitch coefficient with angle of attack for an oscillation amplitude of 2°; $\frac{x_r}{c}$, 0.35; f, 11 cps approx.; RN, 1,250,000.

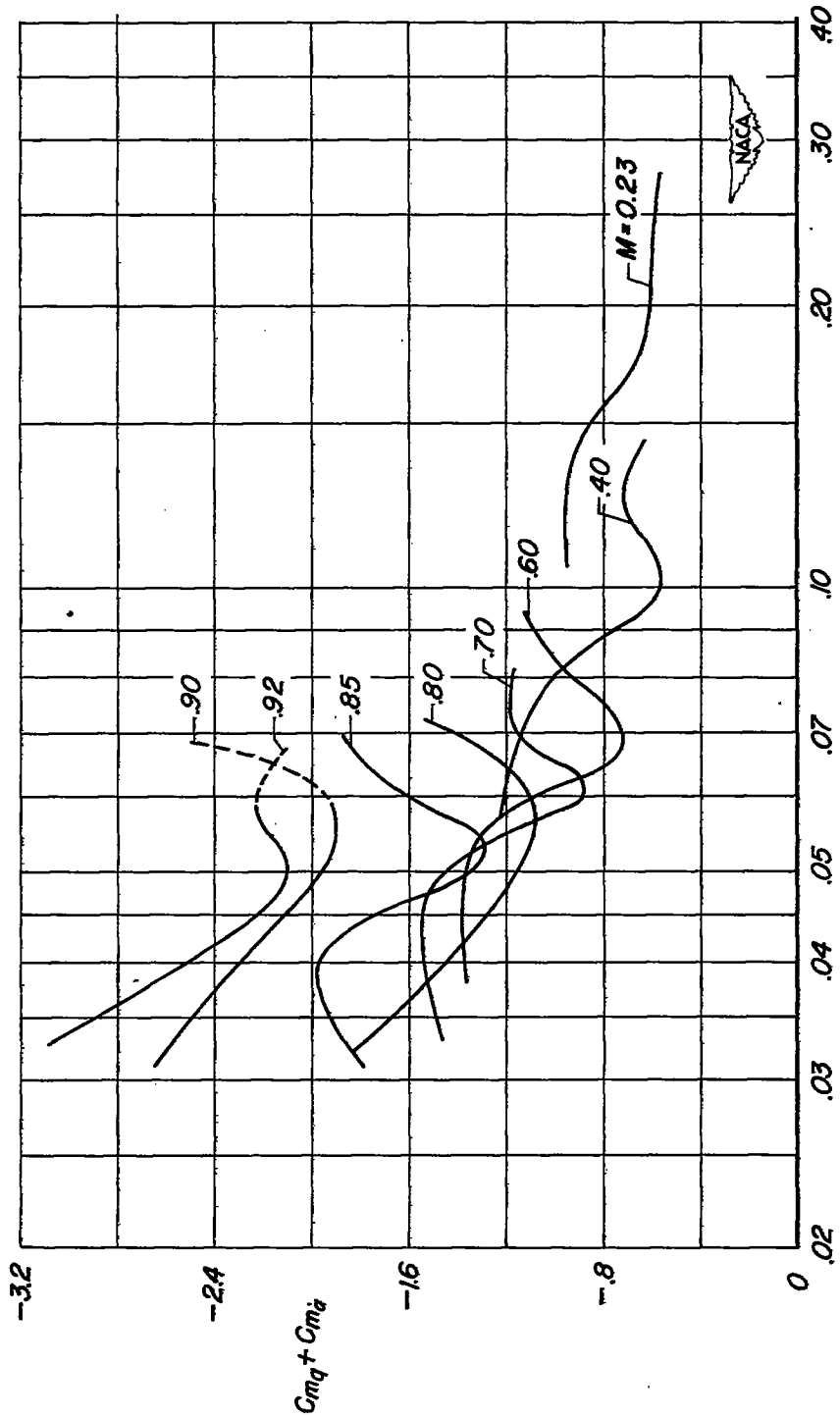

Figure 15.- The variation of damping-in-pitch coefficient with reduced frequency; θ_{max}, 2°; $\frac{x_r}{c}$, 0.35; α_o, 0°; RN, 1,250,000.

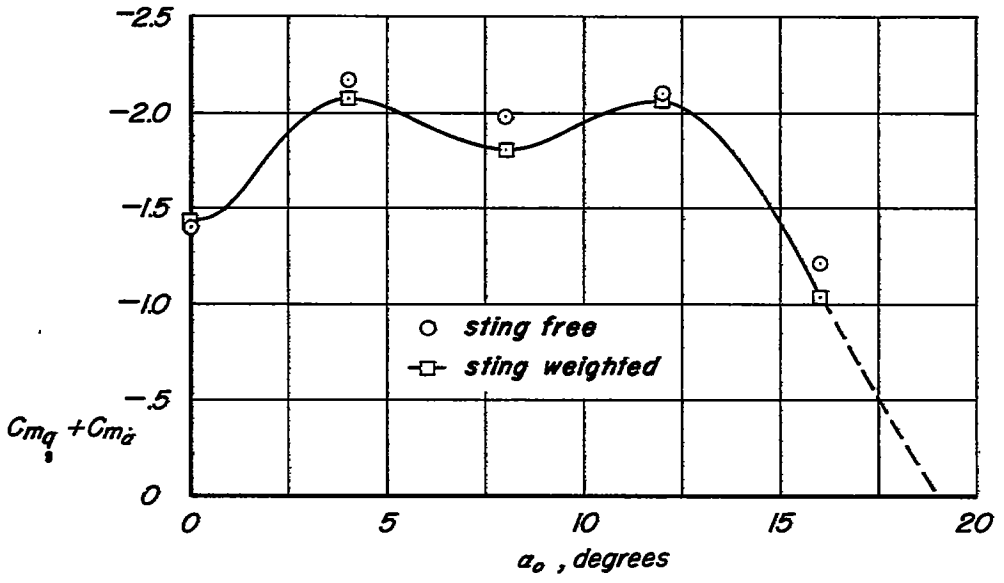

(a) $C_{m_q} + C_{m_{\dot{\alpha}}}$ vs α_o for $M = 0.80$

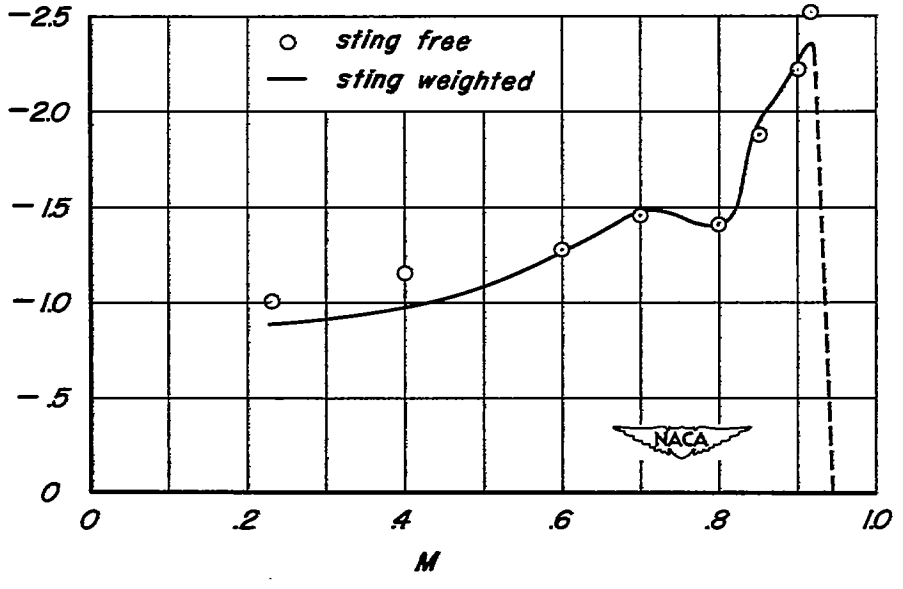

(b) $C_{m_q} + C_{m_{\dot{\alpha}}}$ vs M for $\alpha_o = 0°$

Figure 16.–A comparison of the effect on the damping-in-pitch coefficient of a change in the model–support vibratory characteristics; θ_{max}, 2°; $\frac{x_f}{c}$, 0.35; f, 14 cps approx.; RN 1,250,000.

[redacted]

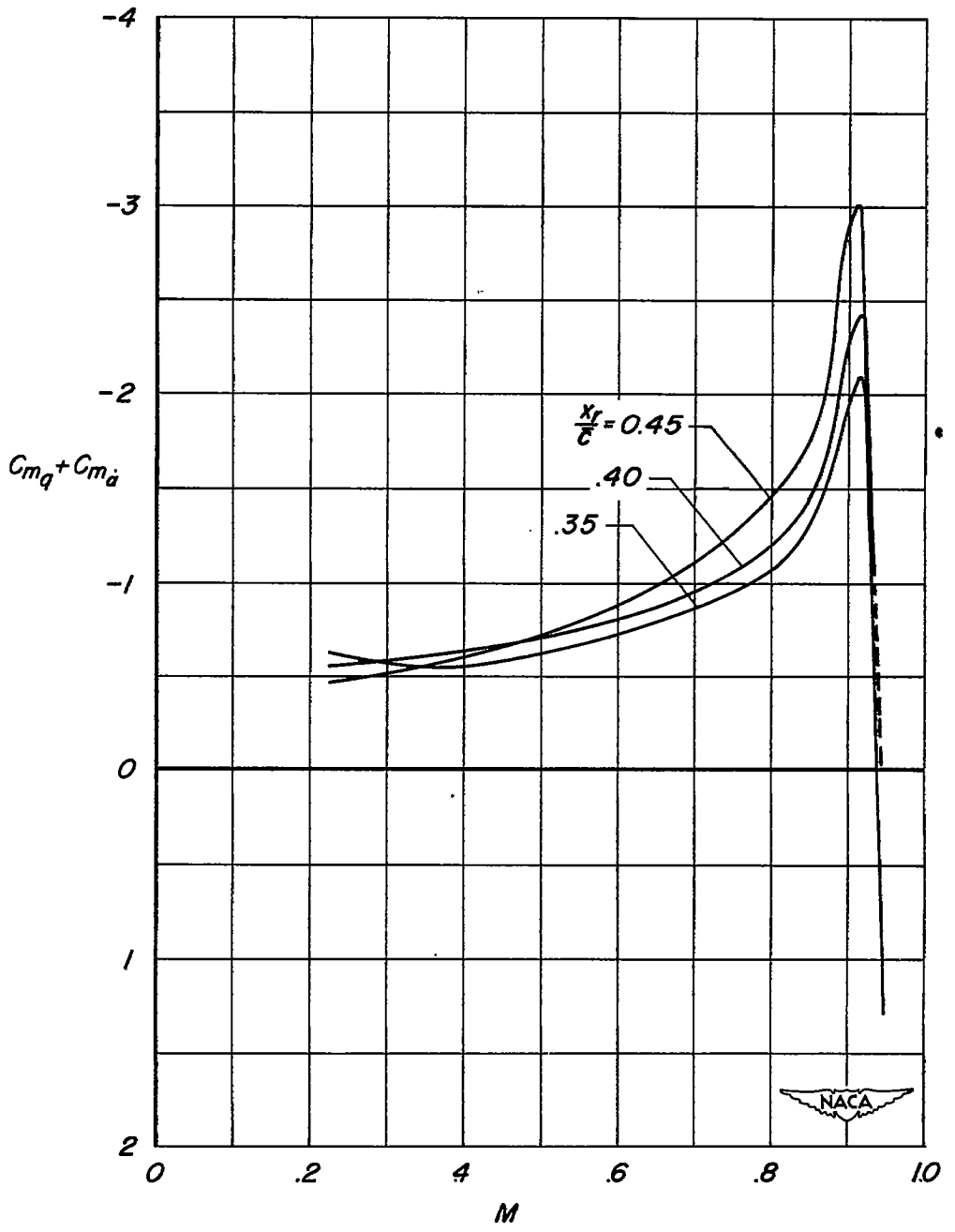

Figure 17.—The variation of damping-in-pitch coefficient with Mach number; θ_{max}, 2°; f, 19 cps approx.; α_o, 0°; RN, 1,250,000.

NACA-Langley - 9-5-52 - 350